BULLETIN 167

GEOLOGICAL SURVEY OF CANADA

DEPARTMENT OF ENERGY, MINES AND RESOURCES

MAGNETIZATION DIRECTIONS IN THE MUSKOX INTRUSION AND ASSOCIATED DYKES AND LAVAS

W. A. Robertson

Canadian Contribution No. 89 to the International Upper Mantle Project

Price $1.50

Ottawa
Canada
1969

MAGNETIZATION DIRECTIONS IN THE MUSKOX INTRUSION AND ASSOCIATED DYKES AND LAVAS

1450-1968-5731-5

Technical Editor
S. JENNESS

Critical Readers
A. LAROCHELLE, N. IRVINE, AND C. FINDLAY

Editor
MARGUERITE RAFUSE

Text printed on NO. 2 ENAMEL

Set in Times Roman with
20th Century captions by
CANADIAN GOVERNMENT PRINTING BUREAU

Artwork by CARTOGRAPHIC UNIT, GSC

GEOLOGICAL SURVEY
OF CANADA

BULLETIN 167

MAGNETIZATION DIRECTIONS IN THE MUSKOX INTRUSION AND ASSOCIATED DYKES AND LAVAS

By
W. A. Robertson

Canadian Contribution No. 89 to the International Upper Mantle Project

DEPARTMENT OF
ENERGY, MINES AND RESOURCES
CANADA

Available by mail from the Queen's Printer, Ottawa,
from Geological Survey of Canada, 601 Booth St., Ottawa,
and at the following Canadian Government bookshops:

HALIFAX
1735 Barrington Street

MONTREAL
Æterna-Vie Building, 1182 St. Catherine Street West

OTTAWA
Daly Building, corner Mackenzie and Rideau

TORONTO
221 Yonge Street

WINNIPEG
Mall Center Building, 499 Portage Avenue

VANCOUVER
657 Granville Street

or through your bookseller

A deposit copy of this publication is also available
for reference in public libraries across Canada

Price $1.50 Catalogue No. M42-167

Price subject to change without notice

The Queen's Printer
Ottawa, Canada
1969

PREFACE

The natural remanent magnetization (NRM) of igneous rocks is used in this bulletin in an attempt to show that variations in the earth's magnetic field in the Middle Proterozoic were comparable to present-day secular variation. It also suggests that at that time the position of Canada relative to the axis of rotation of the earth may have been very different from its position today.

Y. O. FORTIER,
Director, Geological Survey of Canada

OTTAWA, January 3, 1966

BULLETIN 167 — Magnetisierungsrichtungen in der Muskox-Intrusion und in den damit verbundenen Gängen und Laven. Kanadischer Beitrag Nr. 89 zum Internationalen Projekt Oberer Mantel

Von W. A. Robertson

Die Magnetisierungsrichtungen in der Muskox-Intrusion, in den Coppermine-Laven und in den Mackenzie-Gesteinsgängen im nördlichen Kanada sind einander ähnlich und weisen darauf hin, dass im späten Mittleren Proterozoikum der Äquator in meridionaler Richtung durch Zentral-Quebec führte.

БЮЛЛЕТЕНЬ 167 — Направления намагничивания в мускокской интрузии и сопряженных дайках и лавах. Канадский вклад № 89, в Международный проект о верхнем покрове земли.

В. А. Робертсон

Направления намагничивания в мускокской интрузии, лавах Коппермайн и макензских дайках на Севере Канады сходны. Они указывают на то, что во время поздней среднепротерозойской эры экватор проходил меридионально через центральный Квебек.

CONTENTS

Illustrations

MAGNETIZATION DIRECTIONS IN THE MUSKOX INTRUSION AND ASSOCIATED DYKES AND LAVAS

Abstract

Palaeomagnetic results are given from 330 samples taken from 143 sites in the Muskox ultramafic intrusion, the Coppermine lavas, and the Mackenzie dykes of northern Canada. Thermal and electromagnetic laboratory studies indicate the stability spectrum present. Thermal demagnetization experiments suggest that the serpentinized samples, especially those from dunite and picrite, are not stable, whereas a high proportion of the samples from basalt, diabase, gabbro, and pyroxenite are stable. Examples of thermal and alternating magnetic field cleaning of partially stable rock groups are given.

Significant magnetic compass deviations were observed at many sites in the mafic and ultramafic rocks. Magnetic anisotropy tests indicate significant magnetic anisotropy only for rocks that show a visible lineation. Sequences of samples through a sill, the layers of the intrusion, and the lava flows point to cyclic variations in the earth's magnetic field of the same order as those in recent times. A statistical test of directions from both sides of a major shear zone suggests no significant rotation about it. The palaeomagnetic results suggest a deuteric origin for the serpentinization.

Radiogenic ages place the intrusion of the Muskox and the Mackenzie dykes, and the extrusion of the Coppermine lavas in the Middle Proterozoic. The palaeomagnetic results were treated statistically yielding pole positions from five major units. The mean position from these is in the Pacific Ocean at 4.7°N, 191.2°E ($k=90$, $\alpha=8$). A palaeolatitude map for North America for the Middle Proterozoic, using this pole position, shows the palaeoequator passing meridionally through central Quebec.

Résumé

Les renseignements paléomagnétiques qui suivent, résultent de l'étude de 330 échantillons prélevés en 143 points de l'intrusion ultramafique de Muskox, des laves de Coppermine et des dykes de Mackenzie du Canada septentrional. Des études thermiques et électromagnétiques en laboratoire mettent en évidence le spectre de stabilité qui s'y trouve. Les expériences de démagnétisation thermique montrent que les échantillons serpentinisés, particulièrement ceux qui proviennent de la dunite et de la picrite, ne sont pas stables, tandis qu'une forte proportion des échantillons provenant du basalte, de la diabase, du gabbro et de la pyroxénite le sont. L'auteur donne quelques exemples de démagnétisation de groupes de roches partiellement stables sous l'action de la chaleur ou d'un champ magnétique alterné.

D'importantes déviations du compas magnétique ont été observées en de nombreux points des roches mafiques et ultramafiques. Les essais d'anisotropie magnétique ne mettent celle-ci en évidence d'une manière sensible que pour les roches dont le lignage est visible. Les successions d'échantillons d'un bout à l'autre d'un filon-couche, les couches de l'intrusion et les coulées de laves indiquent que les variations cycliques dans le champ magnétique de la terre sont du même ordre que celles des temps récents. Une étude statistique de directions des deux côtés d'une zone de cisaillement de forte intensité n'indique aucune rotation significative qui lui soit liée. Les résultats paléomagnétiques dénoteraient une origine deutérique de la serpentinisation.

Les âges radiogéniques font remonter l'intrusion des dykes de Muskox et de Mackenzie, de même que l'extrusion des laves de Coppermine, au Protérozoïque moyen. Les résultats paléomagnétiques ont été traités statistiquement en utilisant les positions du pôle déduites à partir de cinq unités importantes. La position moyenne ainsi obtenue se situe en un point de l'océan Pacifique dont les coordonnées sont: 4.7° de latitude nord et 191.2° de longitude est ($k=90$, $\alpha=8$). La carte de paléolatitude de l'Amérique du Nord au temps du Protérozoïque moyen, utilisant cette position du pôle, montre que le paléoéquateur passe en direction méridienne par le centre du Québec.

INTRODUCTION

The Muskox Intrusion is a layered body of ultramafic, gabbroic, and granophyric rocks that crosses the Arctic circle and the 115°W meridian in the Northwest Territories of Canada (Figs. 1, and 2 *in pocket*). It was discovered in 1956 during an aerial reconnaissance by the Canadian Nickel Company. The slight northerly dip of the intrusion has caused the whole layered series to be exposed at the land surface. Furthermore recent glaciation has removed much of the weathered material so that the Muskox complex provides fresh samples of what may be differentiated upper mantle material. These factors, combined with the accurate detailed mapping and petrological study of the layers by Dr. C. H. Smith and his associates (Smith, 1962; Smith and Kapp, 1963), have made possible a comparative study of the reliability of the palaeomagnetic results from the various rock groups of this ultramafic–mafic suite, which should prove a useful guide in future palaeomagnetic collections from similar rock bodies.

The detailed palaeomagnetic study of the Muskox Intrusion has used mapped petrological units as palaeomagnetic groups. The Coppermine lavas and Mackenzie dyke swarm were sampled in less detail and each is treated as a single unit. Samples from these groups have been studied in the laboratory in an attempt to determine the direction of the earth's magnetic field relative to the rocks at the time they cooled. A palaeolatitude map (Fig. 19) has been compiled from the results, based on the assumption that the mean direction from the formations is derived from a geocentric axial dipole field at the time the rocks formed (Creer, *et al.,* 1957).

A radiogenic age determination program run in conjunction with the field studies gives a good time basis for the palaeomagnetic results and the palaeolatitude map. Until recent advances made possible consistent ages from whole rock analyses of basic intrusions, most radiogenic ages came from granitic rocks, whereas lavas and sediments have provided most of the palaeomagnetic data. The Muskox layered intrusion is one of comparatively few rock units that may be dated radiogenically and studied palaeomagnetically.

This work was carried out in the Geophysics Division of the Geological Survey of Canada while the author held a National Research Council postdoctoral fellowship.

Dr. C. H. Smith gave helpful co-ordination of the field work with a drilling program at Muskox, and Drs. D. C. Findlay and T. N. Irvine gave much valuable advice both with regard to field exposures and petrological distinctions. Mr. G.

MS. received October 1965.

Dalaire, then a summer assistant at the Geological Survey, helped in collecting the samples.

The laboratory work was carried out in the palaeomagnetic laboratories of the Geological Survey where technicians were made available to do most of the routine measurements and sample preparation. The writer wishes to thank Dr. A. Larochelle for suggesting the project and for his help throughout.

The high sensitivity astatic magnetometer of the Dominion Observatory was kindly made available by Mr. J. L. Roy for the measurement of the most weakly magnetized specimens.

GEOLOGY AND AGE

The Muskox Intrusion, situated in the northwest corner of the Precambrian Canadian Shield, crops out in folded Precambrian basement gneisses and metasedimentary schists (Fraser, 1960; Smith, 1962). The northwest corner of the intrusion is covered by gently dipping sandstone and dolomite of the Hornby Bay Group, of Middle Proterozoic age, which is overlain by the Coppermine lava flows. The many diabase dykes that intrude the basement rocks are part of the Mackenzie swarm (Fahrig and Wanless, 1963).

Muskox Intrusion

The following is a succinct description of this intrusion taken from an abstract by Smith and Kapp (1963):

> A Precambrian layered pluton, 74 miles in length, which is dyke-like in plan and funnel-shaped in cross-section. Its internal structure is divided into four principal units—a feeder, marginal zones, a central layered series, and an upper border zone. The feeder contains bronzite gabbro and picrite in zones parallel to the nearly vertical walls. The marginal zones parallel the walls of the intrusion which dip inwards at angles of 23 to 57 degrees, and grade inward from bronzite gabbro at the contact through picrite and feldspathic peridotite, to peridotite and, in places, dunite. The central layered series is 5,600 feet thick and contains thirty-four main layers of dunite, peridotite, pyroxenites and gabbros which vary in thickness from 10 to 1,100 feet. These layers are nearly flat-lying and discordant to the marginal zones. The upper border zone is less than 200 feet thick and is characterized by an upward gradation from granophyre-bearing gabbro to granophyre.[1]

The olivine-rich bands, particularly the dunite and picrite, have been partly or wholly serpentinized. A sulphide zone, close to the margins of the funnel along much of its length, is evident from the distinctive rust colour where it crops out. The western part of the intrusion has an apparent horizontal displacement of about 5 miles to the south relative to the main eastern part. A northerly trending shear zone separates the two parts (Fig. 2).

[1] Some numbers in this quotation have been modified from the original by more recent data taken from Findlay and Smith (1965).

Dykes

The twenty dykes sampled, five of them twice, form a very small part, both numerically and areally, of the Mackenzie dyke swarm, but both within a single dyke and between dykes of this small sample, variations in composition are noticeable. Nevertheless they appear to be part of a granophyric, quartz-bearing, tholeiitic diabase suite, considerably less mafic than the average composition of the Muskox Intrusion. Many of the dykes in the sampled area follow the north-northwesterly trend of the grain of the basement (Fraser, 1960).

Lavas

The Coppermine lavas conformably overlie dolomite of the Hornby Bay Group (Fraser, 1960), and in places thin sandstone bands are intercalated between flows. More than sixty separate flows, of which twenty-four were sampled for this study, cover a surface area greater than 2,000 square miles and comprise a stratigraphic thickness of more than 5,000 feet. No baked contacts were found but a sandstone interbed was sampled. The flows dip to the north at about 5 degrees. The lavas are tholeiitic basalts. Individual flows typically have scoriaceous, weathered upper and lower parts and a massive centre. The massive central part forms cliffs on the southerly scarp slopes, from which the samples were taken. The sites form an age sequence with the oldest sites (Z,Y) to the south (Roberson, 1964b; Fig. 1).

Age

The Muskox Intrusion is cut by members of the Mackenzie dyke swarm, but the intrusion also appears to cut dykes of this swarm. Likewise dykes cut lower members of the Coppermine flows, but are rare or absent in the upper part of the lava sequence. This field evidence suggests that the Muskox Intrusion, the Mackenzie dykes, and the Coppermine flows may be part of a single Proterozoic phase of igneous activity.

Potassium-argon ages determined from biotite in the sulphide zone (1150 ± 40 m.y., Lowdon, 1961), and whole rock from the granophyre-bearing gabbro in the upper border zone (1095 ± 60 m.y., Wanless, *et al.,* 1965), place the Muskox Intrusion in the upper part of the Middle Proterozoic. Radiogenic ages obtained from the Mackenzie dyke swarm range from 975 to 1360 m.y., spanning the probable time of cooling of the Muskox Intrusion (Burwash, *et al.,* 1963; Fahrig and Wanless, 1963; Wanless, *et al.,* 1965). A flow near the base of the Coppermine lavas yielded a radiogenic age of 1200 m.y. (Wanless, *et al.,* 1965), and one from the middle flows, in the area from which the palaeomagnetic samples were taken, gave an age of 1100 m.y. (Wanless, *et al.,* 1965). Hence, although younger ages have been obtained from other parts of this vast lava sequence (Wanless, pers. com.), it is probable that the age of these flows is similar to that of the Muskox Intrusion.

The difference between the radiogenic ages of the Muskox Intrusion, the Mackenzie dykes, and the Coppermine flows is small, and based on the present data, a late Middle Proterozoic age for the three units is probable.

METHODS

Field Techniques

Two or more oriented samples were collected from each site (Figs. 1 and 2). This was done by selecting a plane surface on the outcrop, scribing a horizontal arrow on it, and measuring its dip with a clinometer. The strike azimuth was

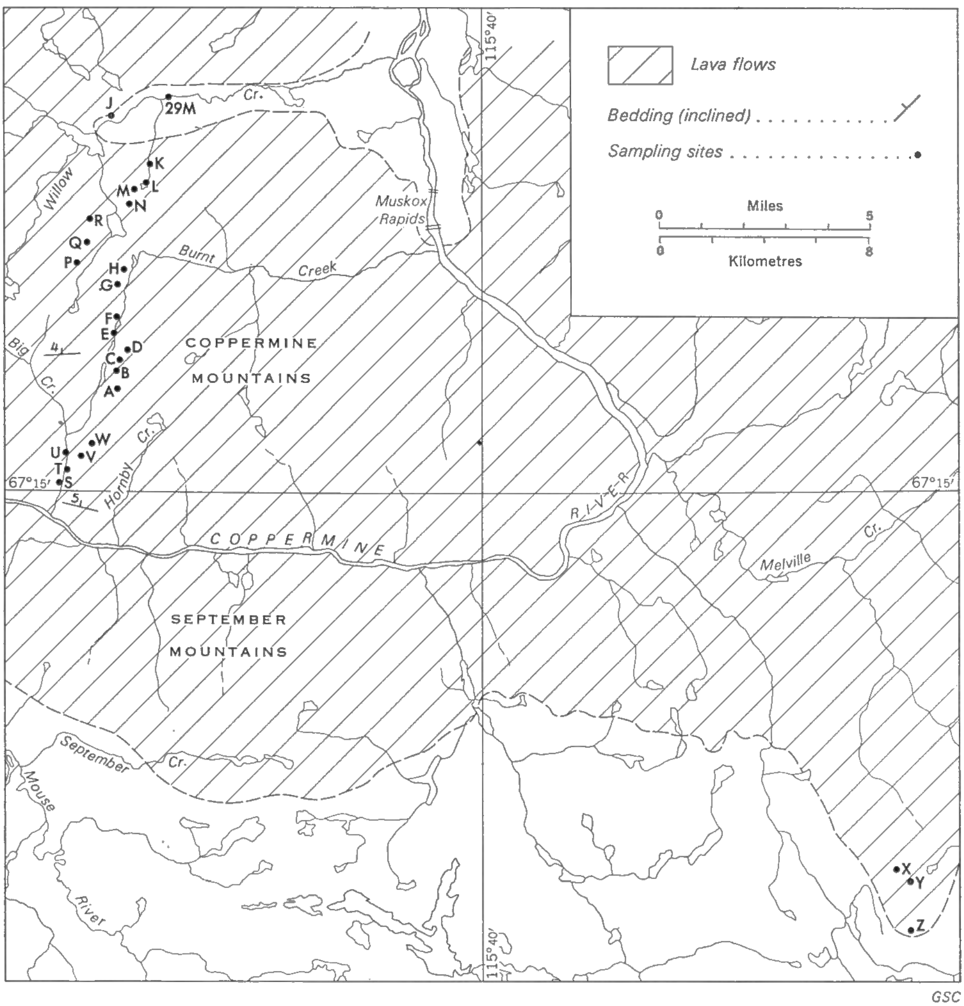

FIGURE 1. Palaeomagnetic sampling sites in the Coppermine and September Mountains lava flows.

measured in each of three ways: i) by placing a Brunton compass on the sample along the strike; ii) by sighting a prismatic compass from a point several feet away from the rock outcrop along the strike line; and iii) by placing the straight edge of a sun compass along the strike line (Larochelle, 1964). In each case the compass was levelled before the reading was taken. The magnetic compasses were adjusted for regional magnetic variation and the sun compass for latitude and apparent solar time. The reading on each instrument is considered to be accurate to the nearest degree if the mean of three readings is used. Thus the attitude of the rock sample, of which the oriented surface is one face, should be known to within 2 degrees. However, appreciably greater discrepancies between readings from different types of compass were found in areas of mafic and ultramafic outcrop. These discrepancies are thought to be due to local distortions of the earth's magnetic field by the magnetic rocks causing local deviations of the magnetic compasses. Hence where solar compass readings were available, they were used.

The size of the error introduced by using magnetic compass readings gives an estimate of the reliability of these readings when the sun compass could not be used because of cloud or shadow. Differences in readings using the Brunton and the sun compass Δ(S-B) for the same sample, and also differences using the prismatic compass and sun compass Δ(S-P), were tabulated for all sites where the sun compass could be used. Figure 3 shows plots of Δ(S-B) as ordinate and Δ(S-P) abscissae for the main rock types. The figure shows that for the ultramafic groups of picrite, pyroxenite, and peridotite, and also for the group of basaltic lavas, errors are commonly 10 degrees or more, and that even for the less magnetic rocks the local average magnetic deviation is nearly twice the probable orientation error of the sample from other sources. The intensity of the horizontal component of the earth's magnetic field in the region where these measurements were made is about 6,000γ; the errors would be smaller in lower latitudes, where this component is larger. The magnetic deviation is controlled by the configuration of the magnetic rock near the sampling station and is likely to be nearly random from sample to sample, so that the probable error for a site mean obtained from two or more samples will be smaller than that for each sample. Differences between sun compass and magnetic compass readings for the main rock types sampled are given in Table I, which suggests the desirability of using sun compass declination measurements wherever possible in high latitudes; it also indicates that when they are unobtainable, the method of standing several feet away from the rock and sighting the magnetic compass along the strike line is the preferable second choice.

The distribution of sampling sites was designed to give a maximum areal and thickness coverage of the formations studied. Effective limits were set by available outcrop and transport facilities. Sample distribution in the *layered*

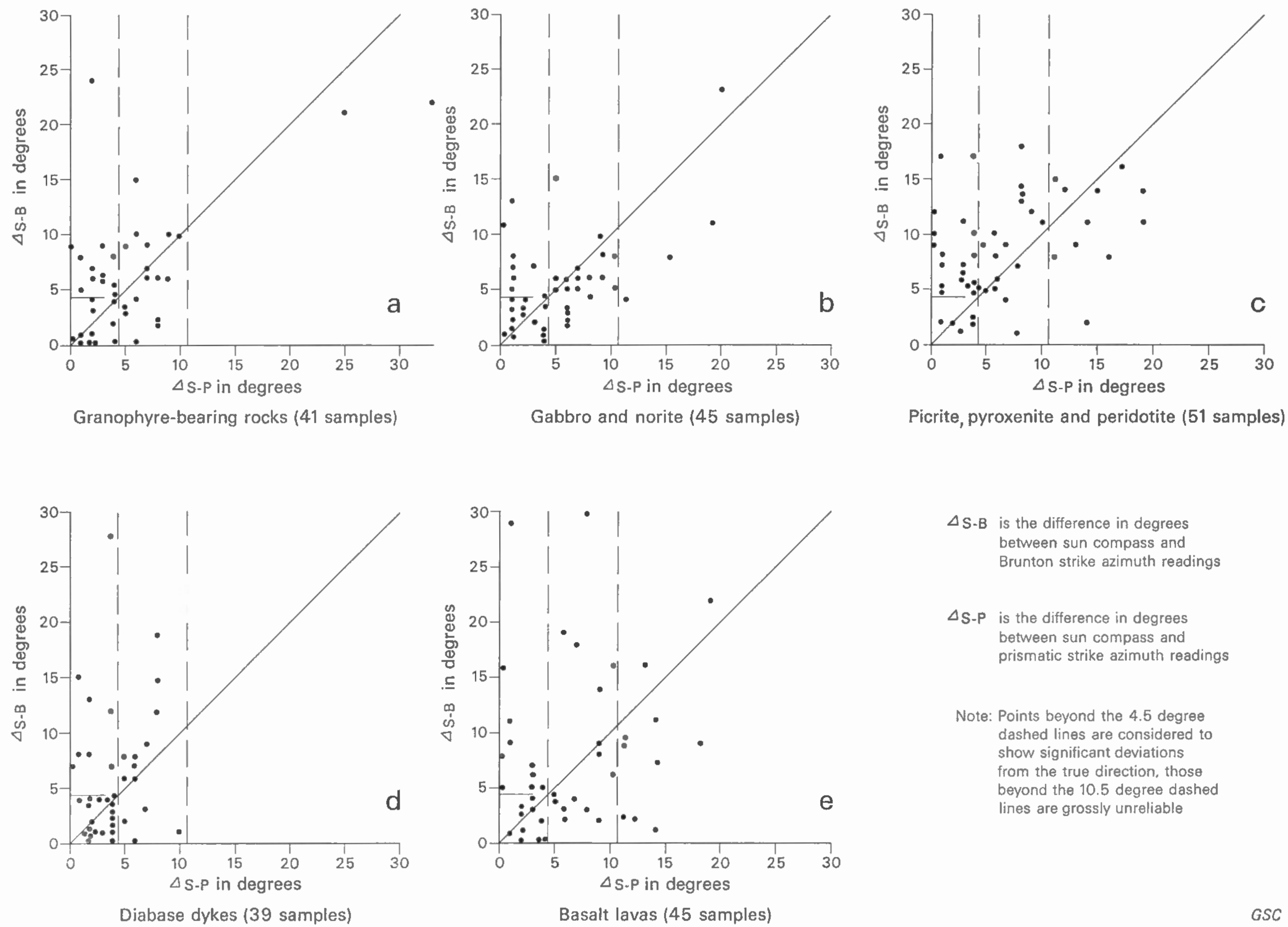

FIGURE 3. Diagrams showing the deviation of prismatic and Brunton compass readings, compared with those made with a sun compass at sampling site composed of different types of basic igneous rock.

series, the *feeder,* the flows, and the sill was also designed to provide information on short term variations of the earth's magnetic field, and the sites in the *central layered series* were closely spaced to allow a comparison of the stability characteristics of the different rock groups.

TABLE I *Deviations of Magnetic Compasses (H is about 6,000γ)*

Rock type	Magnetic minerals	Intensity xn emu x10-6*	No. of sites	No. of samples	Av. Δ(S-P)	Av. Δ(S-B)	%>5° Δ(S-P)	%>5° Δ(S-B)
Granophyre (27)	0–1% Ilmenite Minor hematite	0.1–1	2	4	3	3	25	25
Mafic Granophyre (26)	2–4% Magnetite 2–6% Ilmenite	2–300	5	9	4	5	33	55
Granophyric Gabbro (25)	2–4% Magnetite 2–6% Ilmenite	5–800	4	8	8	7.5	50	60
Granophyre-bearing Gabbro (24)	1–2% Magnetite 1–3% Ilmenite	90–850	10	20	5.5	7	50	65
Gabbro (22)	0–1% Magnetite and magnetite-ilmenite intergrowths 1–2% Ilmenite	80–420	8	19	5	4	60	45
Norite (21)	0–1% Magnetite } 1–2% Ilmenite } Local pyrrhotite	40–550	9	26	5.5	6.5	45	60
Pyroxenite (16a), (16b), (17), (19)	0–0.5% Chromite 0–0.5% Secondary magnetite	5–1400	10	20	6	7.5	50	85
Picrite (15)	0–1% Chromite } 0–1% Ilmenite } 2–8% Secondary magnetite Local pyrrhotite	100–4000	10	20	7.5	9	60	80
Peridotite (12), (13)	1–2% Chromite } 0–1% Ilmenite } 2–12% Secondary magnetite	6–2000	6	11	5.5	9	45	90
Diabase Dykes (29)	2–6% Magnetite and ilmenite	1–6000	19	39	4	6	33	45
Basalt Flows (30)	1–5% Magnetite and ilmenite	500–5800	21	45	8.5	7.5	50	60

NOTE: Av. Δ(S-P) and Δ(S-B) are the average deviation of the prismatic and Brunton compass readings relative to that of the sun compass. The % >5° Δ(S-P) and Δ(S-B) are the proportion of these readings that differ by more than 5° from the sun compass and hence are considered to show significant departures from the true direction.

*Anomalously high intensities, higher by a factor of 10 than the average for the group, have been excluded, as they are considered likely to be due to local lightning strikes and do not reflect the intensity of the rock outcrop as a whole.

Laboratory Techniques

Measurement of Directions

Two cubic specimens of one inch sides were cut from each sample collected in the field. One face of each cube was cut parallel to the oriented surface, with one edge parallel to the orientation arrow. The arrow on this surface was transferred to each cube to preserve the orientation.

The direction and intensity of magnetization of most of the specimens were measured on an automatic magnetometer designed by Larochelle. A computer program also designed by Larochelle was used to calculate the *declination* (D), *inclination* (I), and *intensity* (M) of magnetization from the magnetometer readings. Some magnetization directions were measured on a spinner magnetometer (Larochelle, 1965). Specimens too weakly magnetized to be measured on the automatic magnetometer ($M \leq 2x10^{-6}$emu/cc) were measured on the high sensitivity magnetometer of the Dominion Observatory, Ottawa (Roy, 1963); D,I, and M were calculated from these measurements using a modified version of the above program.

Cleaning

The NRM of rocks is commonly composite (Fig. 4). Igneous rocks acquire a primary component of magnetization (*O*) which is a *thermo-remanent magnetization* (TRM), when they cool in the earth's magnetic field. They may also acquire

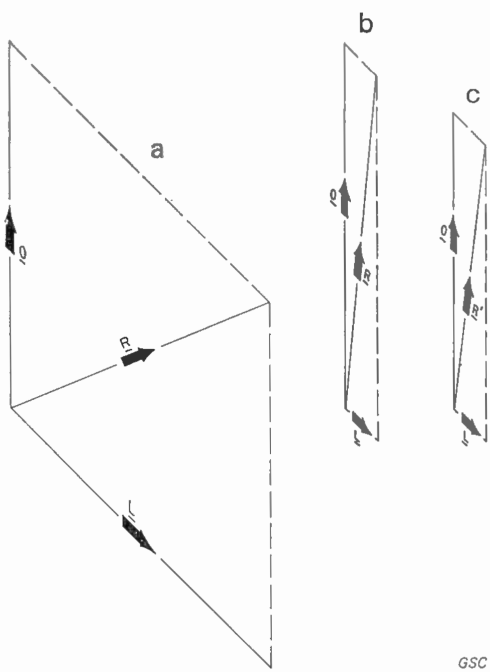

FIGURE 4. Vector diagrams showing resultant (*R*) of original (O) and secondary (*L*) components of magnetization; (a) from a partially stable specimen in which both O and *L* are large; (b) from a stable specimen in which *L* is small; (c) the result of cleaning a specimen that initially gave diagram (a).

secondary components (L) (Creer, 1957) from several sources. The most common of these is a *viscous remanent magnetization* (VRM) (Thellier, 1937) due to low temperature thermal agitations in the earth's field over a long time. Some rocks acquire a *chemical remanent magnetization* (CRM) (Kobayashi, 1959; Howell, *et al.,* 1960; Howell, 1962), during either deuteric alteration or recent weathering processes. Also a rock may acquire an *isothermal remanent magnetization* (IRM), due to a strong magnetic field for a short time, such as that due to a *lightning strike* (Graham, K., 1961; Cox, 1961).

Secondary components have been reduced here both by heating specimens (*thermal cleaning*) and by subjecting another specimen from the same sample to an alternating magnetic field (*magnetic cleaning*). Larochelle (1958) designed the alternating field demagnetizer used. In it an alternating magnetic field is introduced, in the absence of a steady field, along each axis of the cube in turn, maintained for more than 5 seconds and slowly and smoothly reduced to zero. *Thermal cleaning* was accomplished in the non-magnetic oven described by Robertson (1964a), an adaptation of one designed by Irving, *et al.* (1961). The specimens were heated in a nitrogen atmosphere to a given temperature, and cooled in a null field.

Magnetic cleaning and *thermal cleaning* are effective if the *coercivity* or *blocking temperature,* respectively, of the secondary component (L) is less than that of the original component (O). Either technique tends to reduce the intensity of the original component (O), and if the specimens are over-cleaned this will result in an increase in scatter within a homogeneous group (i.e., lavas at Th. 480°C). Both appear to be effective in removing components due to *viscous magnetization* and magnetic cleaning those due to *lightning strikes.* Both may be ineffective against *chemical magnetization* in which the coercivity and the *blocking temperature* are commonly higher than that for the TRM of many igneous rocks. A careful search was therefore made in rock outcrop, hand specimen, and thin section, for possible chemical alteration, commonly weathering, which might cause a secondary component resistant to cleaning.

Statistical Analysis

In order to estimate the reliance that may be placed on the direction obtained from a formation it is necessary to take from it as many samples as practicable and to note the dispersion of the individual directions. Using Fisher's (1953) analysis of dispersion on a sphere one may obtain a mean direction from a group of individual results by giving each direction unit weight and adding them vectorially. Fisher's analysis also provides an estimate of the precision (k) of this mean direction, which is substantially independent of the number of samples (N) used, and the half-angle of the cone of confidence (α) at a given probability. We use $P = 0.05$ and the α obtained is that of a cone inside which the resultant is likely to lie 19 times out of 20. Since α decreases as both k and N increase, many samples must be collected from a formation with a low k to acquire a reliable result. In this study the statistics were computed using a program originally designed by M. A. Ward and modified by A. Larochelle.

These statistics are only valid if errors associated with each unit are independent of each other, and only apply to a whole formation if it has been adequately sampled. Thus many specimens from one sample or one site may give a very high k but an incorrect direction, if all specimens have suffered the same rotation (i.e., by block tilting or hillslip), whereas the same number of specimens, one from each of many sites, may give a lower k, as errors due to sample orientation, tilting, or viscous components are commonly different for each site. The dispersion of samples from one site (ω of Watson and Irving, 1957) may result from collecting and measuring errors, which are commonly random between samples, but linked in specimens from the same sample. The two-tier analysis of Watson and Irving (1957), which isolates collecting and measuring errors, could not be used here because of the wide range of precision between groups. The method adopted is to use sample means obtained from one to five specimens as basic units and to compute site means from them. The site directions have been combined into petrological groups in two ways: 1) Table V gives group means using all sites in each group; and 2) the valid sites of Table VI have to pass Watson's (1956) test of randomness if they contain more than two samples, and sites with only two samples have been rejected if the resultant, R, is <1.75 (angular separation between samples $>$ 1 radian). Group directions have been computed using both samples and sites as units, and the directions in the major units of the Muskox complex have been computed using both sites and groups as units. Comparison of Table V, containing all the data, with Table VI, which gives only valid sites as specified above, shows that Table VI gives higher precision in groups where the vectors are widely scattered, but the mean directions are only significantly changed for groups where all the data give very large error circles.

Palaeomagnetic *pole positions* were calculated from the directions of magnetization (Creer, *et al.*, 1957), again using the program of Ward modified by Larochelle mentioned above. These *pole positions* may be directly compared with those from formations elsewhere in the world since a palaeomagnetic *pole position* is unique for any one dipole field configuration. *Pole positions* were obtained for each group both from sample and site mean directions and also from the mean site *pole positions* (Tables V and VI) and also for each zone (Table VII), the lavas and dykes each being treated as a zone.

LABORATORY STUDIES

The primary object of the laboratory studies described here is to classify the samples into *stable, partially stable,* and *unstable* groups. The unstable group is rejected, and the partially stable group is cleaned, so that the final direction, from the cleaned stable and partially stable groups is close to that of the original field direction (O), acquired as a TRM at the time the rock cooled.

It is also necessary to ascertain that the TRM parallels the direction of the original field. Magnetostrictive effects appear to be small in most igneous rocks (Stott and Stacey, 1959, 1960, 1961; Kern, 1961a,b), and reversible (Stacey, 1960a, 1963, pp. 119–121) that is, rocks subjected to such stresses are thought to assume the field direction when the stress is released; they will not be considered further. Rocks with a visible fabric may also be magnetically anisotropic (Stacey, 1960b), and this anisotropy has been shown to be colinear with the preferred orientation of the fabric (Stacey, *et al.,* 1960). Tests for this effect on the Muskox rocks are described in a later section.

Thermal Demagnetization

Specimens may be heated in a null field to some temperature below the Curie temperature, thus separating high from lower temperature components of NRM, or they may be heated above the Curie temperature and cooled in a known field, thus acquiring a laboratory TRM, of which the various temperature components may be studied. These two techniques, used on Muskox material, are described and compared.

Thermal Demagnetization of NRM

Sets of three to five specimens from different sites for all the main rock groups were heated in the non-magnetic oven and cooled in a null field. Directions and intensities of magnetization were measured after cooling. The temperature to which specimens were raised was increased by steps up to 600°C or until the intensity ceased to decrease.

Curves of normalized mean intensity of NRM $\left(\frac{M}{M_o}\right)$ versus temperature are shown in Figure 5. More than half of the NRM of the gabbroic, dyke, and lava groups, thought to be stable from the direction criteria, resides in minerals with blocking temperatures over 500°C, whereas the blocking temperature range for the picrite, dunite, and websterite groups is much wider. The wide scatter of some of the points for the picrite and dyke curves may be due to the heterogeneity of these groups.

Figure 6 shows curves of the parameter $\frac{k}{k_{sig}}$ (where k_{sig} = (N–1)/(N–Ro), and Ro is Watson's (1956) resultant of N random vectors at P = 0.05 (Irving, *et al.*, 1961)) for the same rock groups, plotted against temperature. The large errors possible in k due to the small sample size, combined with wide temperature spacings, allows much latitude in the drawing of some of the curves, which also are not always typical of the groups they represent. The lava group curve is an example (Table IV); the very low initial precision is due to the inclusion of an erratic direction from one partially stable specimen out of three. Also the high precision for the dunite

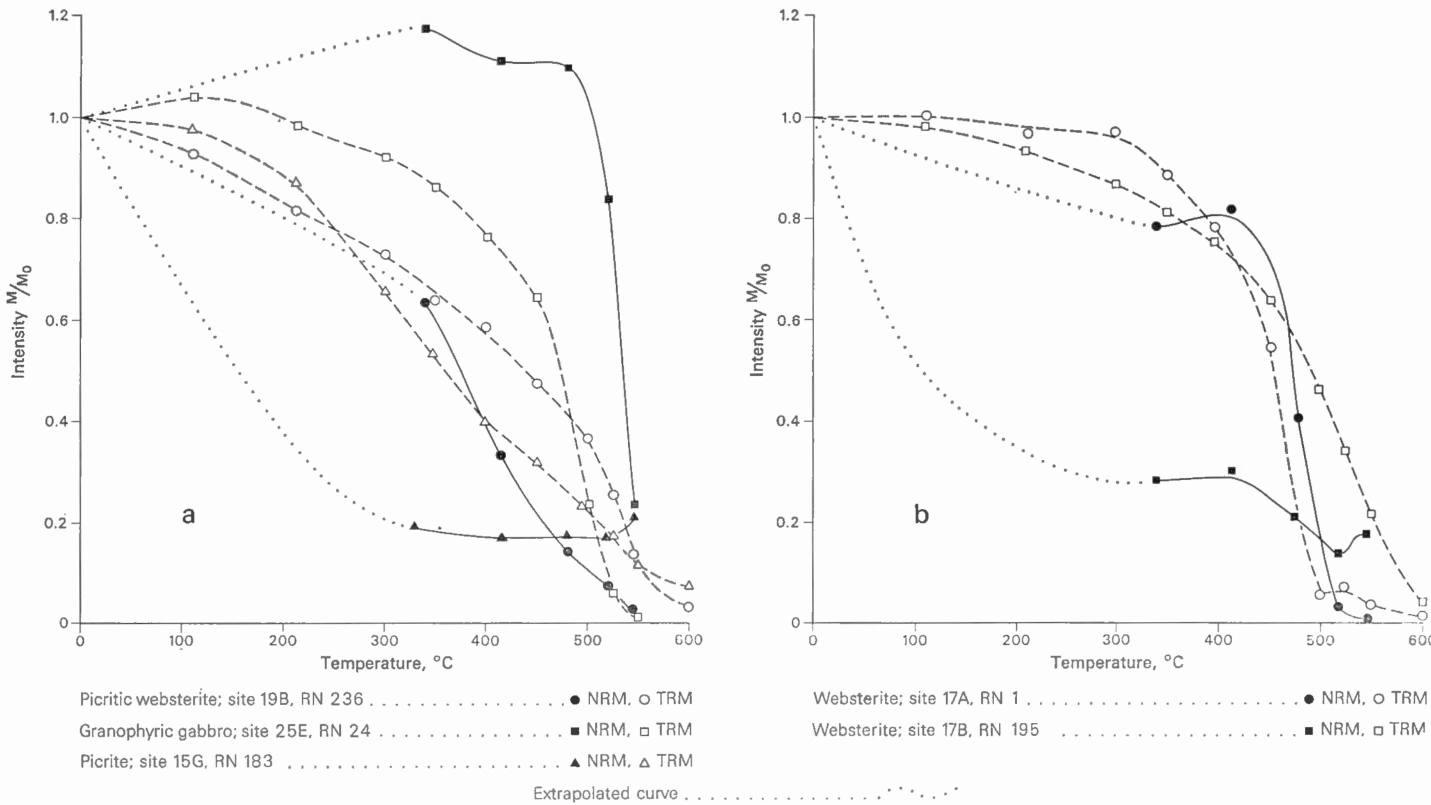
a
b
Intensity M/Mo
Temperature, °C
Picritic websterite; site 19B, RN 236 ● NRM, ○ TRM
Granophyric gabbro; site 25E, RN 24 ■ NRM, □ TRM
Picrite; site 15G, RN 183 ▲ NRM, △ TRM
Websterite; site 17A, RN 1 ● NRM, ○ TRM
Websterite; site 17B, RN 195 ■ NRM, □ TRM
Extrapolated curve

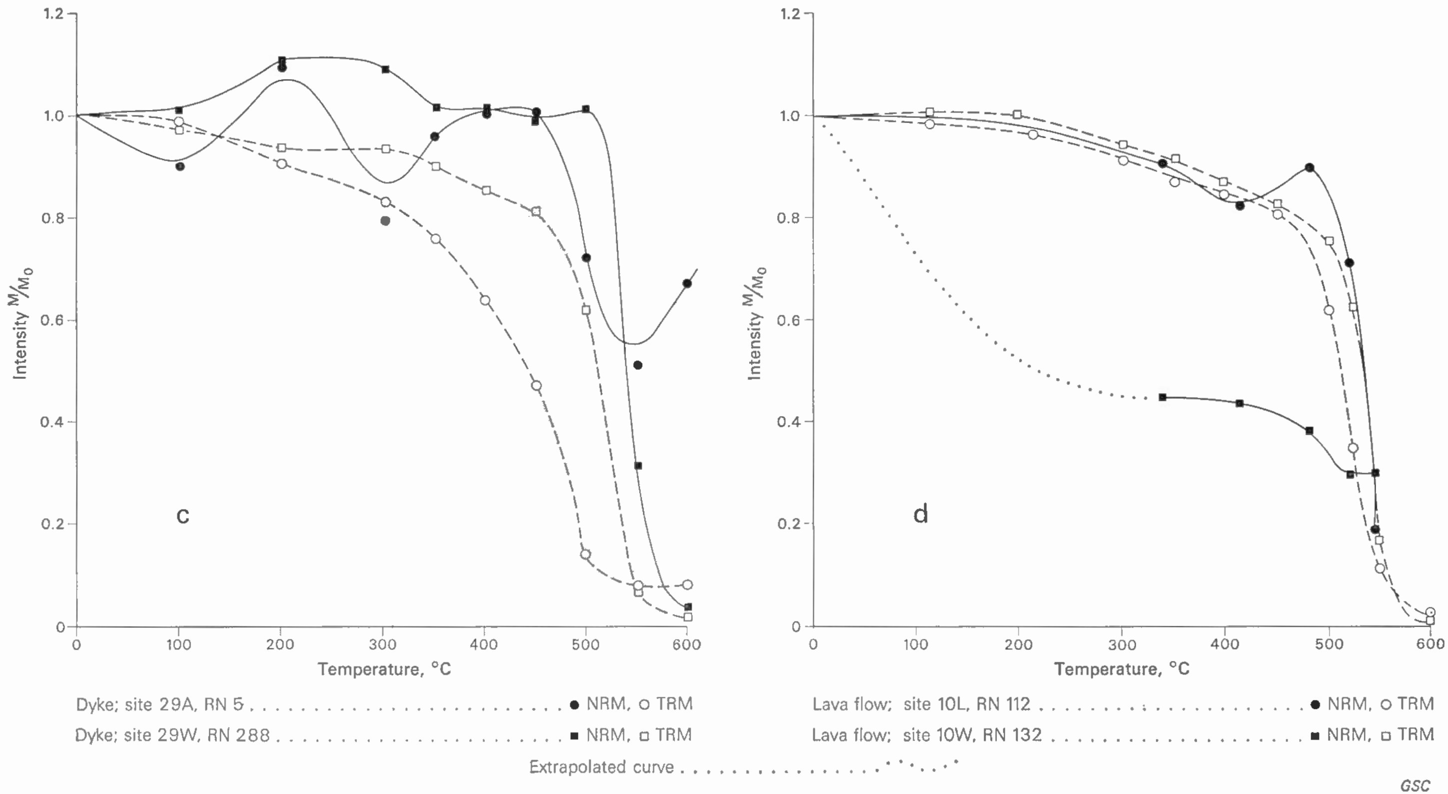

FIGURE 5. Thermal decay of NRM and TRM: normalized intensity as a function of temperature.

is due to the selection of favourable declination values from drill core samples, and is only included to show that the precision remains essentially constant until the specimens are heated above 550°C. Nevertheless, certain broad features are apparent:

1. The precision for each group does not change significantly in the temperature range 300° to 450°C.

2. The precision after thermal cleaning at a temperature greater than 300°C is significantly increased above the initial precision for some groups.

3. There is a wide range of group precisions and for the picrite directions remain random at P=0.05 (Watson, 1956).

These curves suggest that heating the specimens to some temperature between 300°C to 450°C gives effective *thermal cleaning*. Hence one specimen from each sample was heated above 300°C and the statistics from these results are given in Table IV. Detailed tests for each site would reveal more accurately the optimum cleaning temperature, and might possibly reveal higher temperature secondary components; however, it probably would not significantly increase the precision of the results.

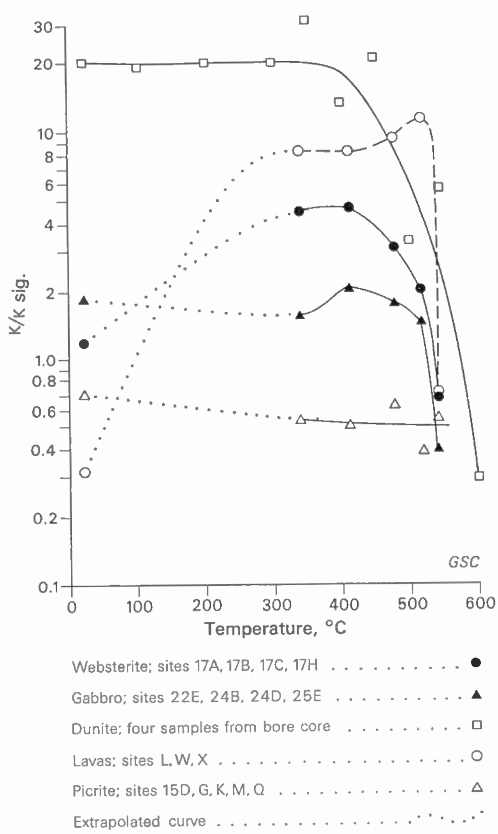

FIGURE 6. Thermal demagnetization of NRM: variation of normalized precision $\frac{k}{k_{sig}}$ as a function of temperature.

Thermal Demagnetization of Applied TRM

Specimens that had been thermally demagnetized were heated above 600°C and cooled in a steady field of 1.1 oe, by reversing the current in the vertical coils nulling the field in the oven. They were then thermally demagnetized by steps. The average relative intensity $\left(\frac{M}{M_o}\right)$ curves for the main groups are shown in Figure 5. These curves are much smoother than their NRM counterparts as the intensity is due entirely to the applied TRM, and is freed from viscous components. Precision curves of $\frac{k}{k_{sig}}$ plotted against temperature are shown in Figure 7. The Curie temperature of the dominant magnetic mineral in the rock has been estimated from each set of curves (Robertson, 1963a) and is given in Table II. The lava, picrite, peridotite, and dunite groups, and probably also the gabbro and dyke groups (Table II and Fig. 7) contain magnetic minerals with Curie temperatures in the range 500° to 570°C. This is consistent with nearly pure magnetite (Akimoto, 1955, 1957; Nicholls, 1955; Vincent, *et al.*, 1957). Chromite, which is the most common opaque mineral in some of the ultramafic rocks, does not appear to contribute significantly to their magnetic properties.

TABLE II | *Estimation of Curie Temperatures*

Rock group	CT in °C from TRM precision curve, Fig. 6	CT in °C from TRM intensity curve, Fig. 7	CT in °C from NRM precision curve, Fig. 5	CT in °C from NRM intensity curve, Fig. 7
Lavas	550–580	525–560	525–550	500–575
Dykes	525–550	450–540	—	500–560
Gabbro	530–580	460–530	525–550	525–550
Websterite	500–525	475–570	525–550	400–520
Picritic websterite	—	450–550	—	350–525
Dunite	510–540	—	550–600	—

Comparison of NRM and TRM Thermal Demagnetization

Oxidation during thermal demagnetization is kept to a minimum both by heating in a nitrogen atmosphere (Robertson, 1964a), by maintaining the maximum temperature only long enough to ensure thermal equilibrium (about 5 minutes), and by the removal of the insulating jacket, allowing rapid cooling (Irving, *et al.*, 1961).

Samples in which the curves of intensity for NRM and applied TRM coincide are likely to have acquired their NRM as a TRM when the rock cooled, and parallelism in the higher temperature ranges is thought to indicate partial stability giving primary (TRM) directions in this range. Comparison of the TRM and NRM curves of Figure 5 shows general agreement for the specimens with stable directions, and a parallel tendency in the 300° to 450°C range for the partially stable specimens (compare Robertson, 1963b, Fig. 7(d)).

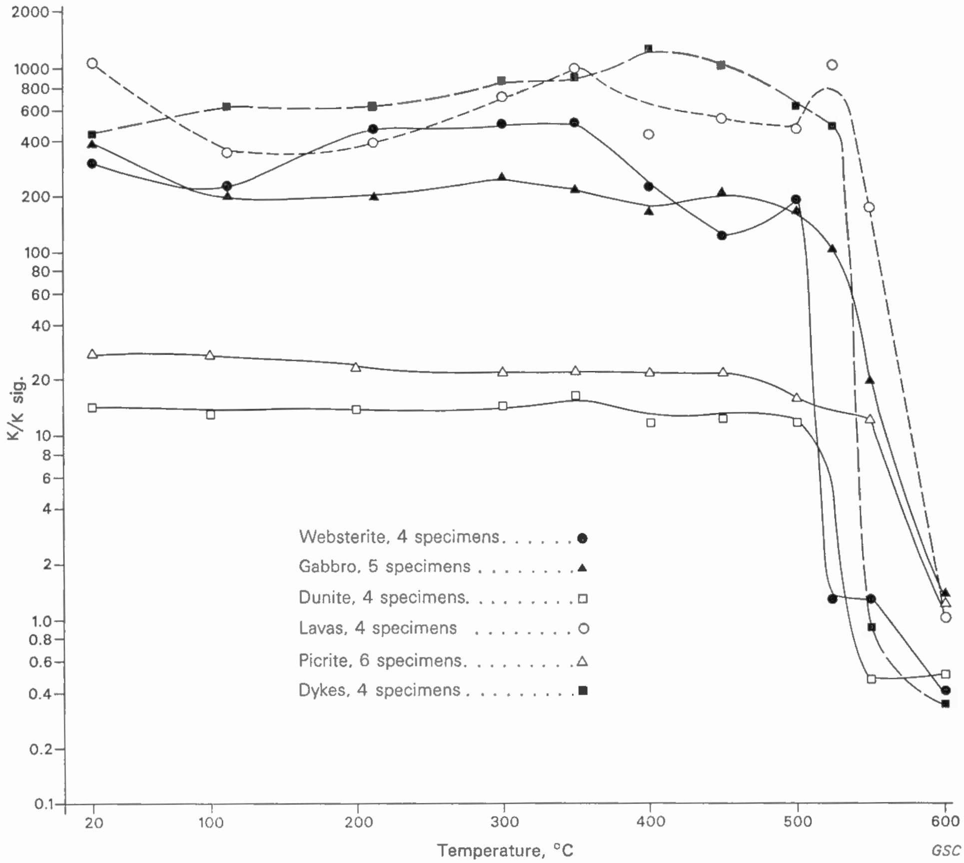

FIGURE 7. Thermal demagnetization of TRM: variation of normalized precision $\frac{k}{k_{sig}}$ with temperature for selected rock groups. The specimens were first given a TRM by heating to 625°C and cooling in a magnetic field of about 1.1 oe, and then demagnetized by steps.

Constant precision (parallel to the temperature axis in Figs. 6 and 7) denotes no scattering components within that range. The much lower precision of the NRM is due both to the lower intensity caused by decay, to collecting and cutting errors that are absent in TRM studies, and to residual secondary components.

A detailed comparison of relative intensities $\left(\frac{M}{M_0}\right)$ for specimens in which both NRM and applied TRM have been thermally demagnetized is shown in Figure 5. Figure 5 shows characteristic pairs of curves from stable (RN236) and unstable (RN183) specimens. Curves from partially stable specimens show a wide variation; NRM intensity values such as those for specimen RN24 that are greater than the TRM values suggest: (1) the primary component is in a direction opposed to the secondary component, which is preferentially removed, causing an increase in the NRM vector, or (2) preferential decay of the low temperature components of NRM during geological time, or (3) some chemical mixing during heating causing a spread in the blocking temperatures of the magnetic minerals for the applied TRM curve. Curves such as that for specimen RN195 (Fig. 5b), with a rapid intensity decay at low temperatures for NRM only, are commonly due to the preferential removal of a dominant secondary component. Where the precision parameter, k, increases for a group the secondary components are thought to have been preferentially removed.

Magnetic Anisotropy

Magnetic minerals such as magnetite and pyrrhotite are easily magnetized along certain crystallographic axes (Stacey, 1960b; Fuller, 1963). If the axes are preferentially aligned in the rock it may acquire a magnetization direction at an angle to the magnetizing field (Stacey, *et al.,* 1960; Fuller, 1960, 1964).

To test the importance of this anisotropy effect in the Muskox rocks, specimens from each of the main groups were heated above 600°C and cooled in a field of 1.1 oe in a known direction. Deviations from this direction are shown in Figure 8. Deviations were less than 4 degrees for most specimens and were not significant. Four picrite specimens and one each of picritic websterite, peridotite, and dunite produced deviations greater than 10 degrees. Magnetic anisotropy appears to have been a contributing factor in the dispersion of directions of these four rock types. The specimens that exhibited this anisotropy contained a visible lineation. All samples that appeared in hand specimens to be isotropic had negligible magnetic anisotropy.

Change of Direction with Heating

The change in direction of NRM of an individual specimen with increasingly severe treatment gives an alternative criterion of stability to that of the precision (k) of a group. If direction changes are small between each of several increases of temperature or alternating magnetic field then no significant deviating component is removed within this range. Hence for stable specimens direction changes will be small until the blocking temperature or critical field is reached. Partially stable specimens will display rapid changes followed by a plateau of little change. Unstable specimens will show large changes after each treatment.

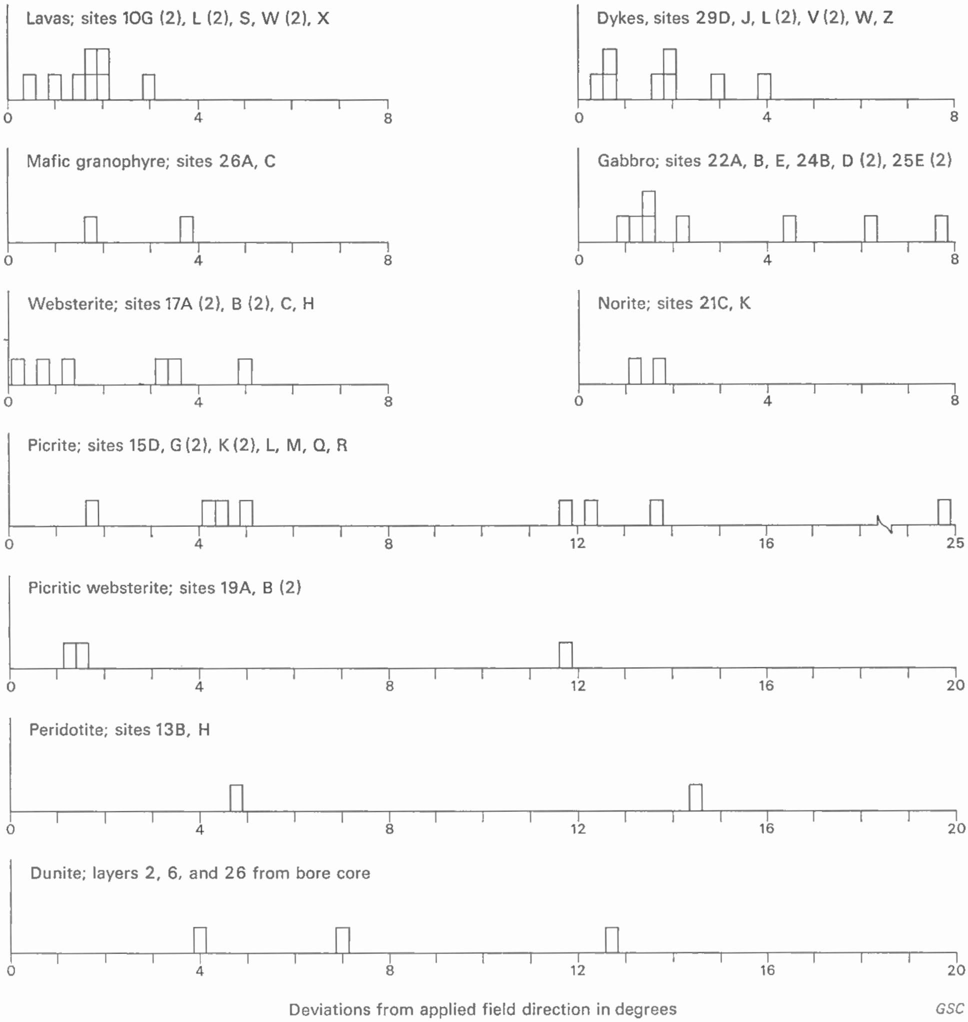

FIGURE 8. Anisotropy of TRM. Deviations from the applied field direction of the magnetization in selected specimens from the main groups of the Muskox Intrusion, the lavas, and the dykes.

Changes of direction after successive heat treatments for individual specimens from most of the groups studied are given in Table III. Using this stability criterion gives qualitative results, which are broadly consistent with that of the precision of the group (Fig. 6). The table illustrates that for most groups, with the exception of the sulphides, there is little change between 300° and 450°C, as indicated by the precision curves (Fig. 6).

Table III also indicates that although some rock types tend towards high stability and others low, there is a wide range of stability within some of the rock groups; selective, post-cooling chemical alteration is the most likely cause. Careful selection of unaltered samples is essential if the direction of the earth's magnetic field at the time of cooling is to be ascertained.

Alternating Magnetic Field Cleaning

Parallel with the *thermal cleaning* another specimen was taken from each sample and submitted to an alternating magnetic field of peak value 75 oe. Directions from these results are given in Tables IV, V, and VI. Higher alternating fields were not used, except for the sill and sulphides, because of the possibility of introducing anhysteritic components using the three-axis, non-rotating method of cleaning.

Comparison with the results of McElhinny and Gough (1963) from the Great Dyke of Southern Rhodesia, also composed of mafic and ultramafic intrusive rocks, suggests that maximum results in some cases might be obtained in alternating fields of peak value greater than the 75 oe used here; such treatment, using alternating magnetic field equipment that will give the necessary homogeneous high fields, might form a future project that could increase the precision of the *magnetically cleaned* results.

In samples from the sill and the sulphide zones, for which higher alternating magnetic fields were used, each specimen was cleaned twice in the same peak field, being placed in the field in the opposite direction the second time. The specimen was measured after each cleaning, and the mean of the two results used; the differences between the two directions was usually less than 10 degrees of arc.

Other Tests

Baked Contacts

The fold and conglomerate tests devised by Graham (1949) give incontrovertible evidence that the NRM was acquired at a time prior to the formation of the conglomerate or the folding. Unfortunately at Muskox neither conglomerates nor folded rock is present. Another powerful test uses rocks baked by an intrusion (Bruhnes, 1906). If the NRM from such baked contacts is in the same direction as that from the intrusion, but different from that in the unbaked country rock away from it, the conclusion is that the direction was acquired as a TRM at the time of cooling.

The intrusion of the Muskox complex did not cause extensive baking of the surrounding country rock which consists mainly of metamorphic rocks in which baking caused only slight apparent alteration. However, samples of metamorphic rocks baked by the Muskox Intrusion were collected from five sites. Scatter of directions from these samples was fairly large, partly because of very low intensities

TABLE III *Changes in Direction between Heat Treatments*

Temperature range through which direction change has taken place, in °C

Site	Sample	I–100°	I–340°	I–415°	100°–200°	200°–300°	300°–350°	350°–400°	340°–415°	400°–450°	415°–480°	450°–500°	480°–520°	500°–550°	520°–545°	550°–600°
LAVA FLOWS																
10G	RN102		4						4		4		5		13	
10L	RN112		93						5		5		9		84	
10W	RN132		33						2		7		2		23	
10X	RN276		12						4		4		3		16	
DYKES																
29J	RN67		10						3		5		26		22	
29L	RN72		3						1		1		1		1	
29V	RN280		15						4		3		6		29	
29Z	RN310			3							1		2			
29A	RN5	8			4	11	8	20		18		45		66		20
29W	RN288	4			1	2	4	4		5		2		20		81
GRANOPHYRIC GABBRO																
24B	RN243		6						0		1		12		74	
24D	RN271		18						30		11		15		121	
24L	RN304		24						9		6		5		63	
25E	RN24		8						7		4		8		116	
GABBRO AND NORITE																
22E	RN258		15						5		1		19		24	
21E	RN173		2						3		2		1		19	
WEBSTERITE																
17A	RN1		3						1		2		5		59	
17B	RN195		27						8		16		21		36	
17C	RN255		24						7		10		45		84	
17H	RN242		31						10		27		16		55	

PICRITIC WEBSTERITE															
19B RN236		3						2		9		24		110	
PICRITE															
15D RN48		59						22		50		95		66	
15M RN155		13						2		0		10		13	
15G RN183		21						7		7		6		18	
15K RN4		39						13		16		20		94	
15Q RN43		3						2		3		8		16	
15N RN11	98			18	1	1	1		2		7		13		120
15B RN13	4	(I–300°) ↓		10	18	16	20		3		10		15		49
15C RN41		29				9	10		14		39		50		10
15F RN60		22				17	12		52		19		10		26
FELDSPATHIC PERIDOTITE															
L20 N1895	6			5	2	(300–400) 6			2		4		2		21
DUNITE															
L14 N2304	2			3	3	3			3		2		2		129
L12 N3184	18			1	2	0			4		28		28		135
L3 S2335	6			3	2	7	9		13		2		22		7
L21 N1708		9						2		3		10		2	
L5 S2182		1						1		3		3		4	
L1 S2820		4						4		4		4		10	
SULPHIDE ZONE															
SA RN204.3	2			7	19	64	36		60		104		102		70
SA RN204.4				4	14	69	60		30		22		4		15
SA RN205.3	2			0	4	128	44		43		108		98		22
SA RN205.4				3	12	82	50		79		36		44		33
SB RN233.3	12			12	26	64	69		30		36		60		112
SB RN233.4	28			19	140	48	128		70		123		102		108
SB RN224.1	63			137	105	92	81		119		130		126		146
SB RN224.2	19			40	67	34	85		108		104		20		48

Site numbers that start with L are layer numbers of specimens taken from bore core resulting in large measurement errors, and was not improved by cleaning (with the exception of thermal cleaning at 310°C at site 30C; *see* Table IV), but the resultant direction is in good agreement with that from the intrusion.

Sulphide Zone

Four samples, two from each of two sites in sulphide zones, were studied in detail, in an attempt to assess the reliability of such rocks for palaeomagnetic work, and to obtain information on the relative age of the intrusion of Muskox and the formation of the sulphide zone. The results showed that the samples were unstable so that they gave no information on relative age.

The two sites from which the sulphide samples were taken exhibited different magnetic characteristics, but neither gave NRM directions that corresponded with those from the Muskox Intrusion. At site SA steep southwest directions were retained with small scatter, after treatment in peak alternating fields up to 125 oe and temperatures up to 300°C; heated above 300°C the scatter became large and directions changed rapidly with temperature (Table III). At site SB a moderate initial scatter increased rapidly after treatment in peak fields greater than 150 oe and temperatures greater than 100°C.

The large changes of direction between heat treatments above 200°C for site SB and 300°C for site SA suggest total instability in the higher temperature ranges. The predominant magnetic mineral in this sulphide zone is known to be pyrrhotite (J. A. Chamberlain, pers. com.) and it seems probable that the random direction changes after heating in the higher temperature ranges are due to random magnetization acquired by the pyrrhotite, heated above its Curie temperature, masking any residual NRM from magnetic minerals with higher Curie temperatures.

Demagnetization curves for both sites are shown in Figure 9a. The TRM curve for site SA indicates a range of blocking temperatures consistent with that for pyrrhotite. The TRM curve for site SB indicates a wider range of blocking temperatures and the presence of a magnetic mineral with a Curie Point higher than that of pyrrhotite. The rise of intensity at low fields and temperatures followed by a rapid fall may be explained by the magnetic interaction of minerals with opposed components at site SB. The low NRM intensity at both sites at 300°C followed by a rise suggests that an initially dominant component has been neutralized at this temperature, and that an initially minor component in an opposed direction may be dominant at 350°C. These components may be due to a pair of magnetically interacting minerals which may theoretically produce a self-reversal (Neél, 1955). The rapid rise of intensity for site SB (Fig. 9b) with peak alternating field treatments between 75 and 150 oe shows that *cleaning* in higher fields might reveal a direction masked throughout the treatment given here.

The conclusion is that the sulphide zone specimens are unstable under the given test conditions, and unless more stringent tests are developed similar sulphide zones are unlikely to give the magnetic field direction at the time of cooling.

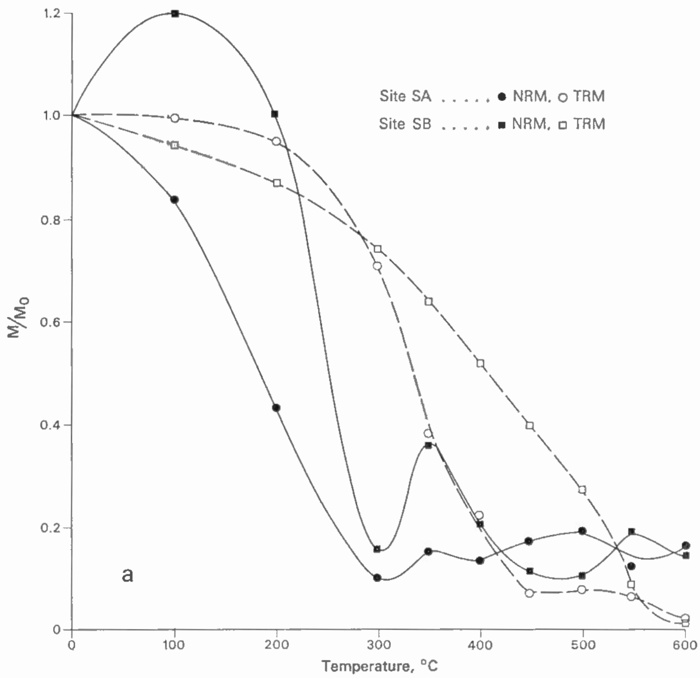

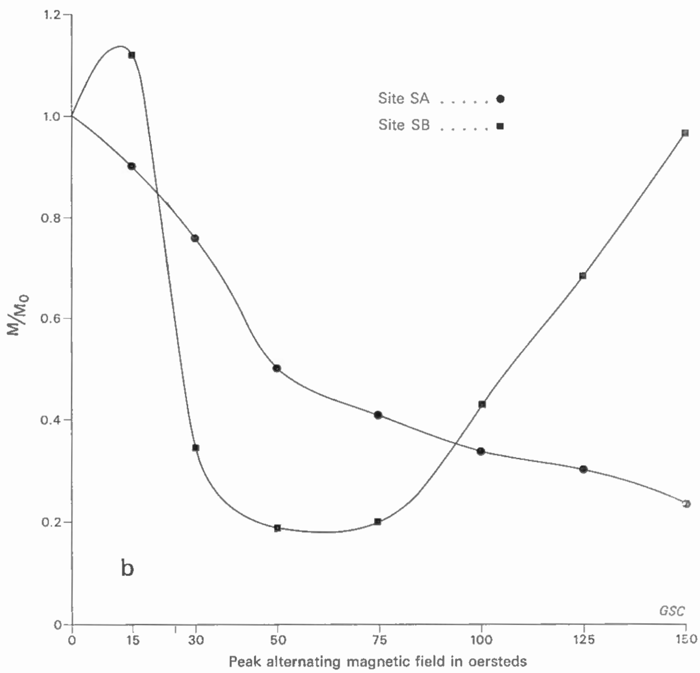

FIGURE 9a. Thermal decay of NRM and TRM for sulphide zone rocks. Normalized intensity $\frac{M}{M_o}$ as a function of temperature.

FIGURE 9b. Alternating magnetic field decay curves of NRM for the same specimens as Figure 9a.

Secondary Alteration

Many of the more mafic units of the Muskox Intrusion have suffered hydrous alteration, mainly of olivine to serpentine and magnetite. In the dunites this reaction is virtually complete, and no olivine remains, whereas picrite, olivine-pyroxenite, and olivine-gabbro show various stages in the breakdown of olivine. It is of interest to ascertain whether the alteration occurred at a late stage in the crystallization of the magma, or whether it is a more recent event.

The magnetite of the dunite is almost entirely of secondary origin whereas in the other olivine-bearing rocks the percentage of primary to secondary magnetite ranges from 0 to 100. The possible types of magnetization for this magnetite are: (1) TRM frozen into the primary magnetite at the time of cooling; (2) CRM in the secondary magnetite formed during chemical reactions during a late stage of the cooling; (3) CRM acquired by the formation of secondary magnetite during chemical alteration at some time after the intrusion cooled; and (4) an *isothermal remanent magnetization* (IRM) due to *viscous magnetization* or lightning, built up in both primary and secondary magnetite. Types (1) and (2) would give NRM directions parallel to the magnetic field at the time the rock formed, whereas the directions associated with types (3) and (4) would align along a more recent field direction. The relatively low coercivity of the IRM of (4) would allow preferential removal of it by *magnetic cleaning,* and the most likely direction of an IRM component would be that of the dipole field (0, + 77), due to the recent build-up of viscous components, with a much steeper inclination than that given by the NRM of stable units of Muskox (238, + 34). Types (1) and (2) are magnetically indistinguishable, but they are obviously petrologically distinct, and easily distinguished. Thus types (1) and (2) may be distinguished from types (3) and (4) by their NRM directions, (1) from (2) petrologically, and (3) from (4) by laboratory tests.

Mean NRM directions of the olivine-bearing groups before and after magnetic and thermal cleaning are shown in Figure 10. All surface samples of dunite were strongly weathered and only inclinations from drill core samples were available. The mean inclinations for the dunite are shown as circles concentric with the centre of the diagram. Initial directions for both picrite and dunite are close to that of the present field direction; after magnetic and thermal cleaning, directions from both groups are farther from this direction, but the large scatter within these two groups suggests that the change may not be significant. Magnetic cleaning of the olivine-clinopyroxenite caused a very wide scatter and an anomalous mean, but the mean for thermal cleaning has moved towards that for the stable groups. The mean for the olivine-gabbro group is near to that for the stable groups but after magnetic and thermal cleaning it is about 15 degrees of arc farther from the present dipole field direction.

The results from the olivine-bearing groups are widely scattered and appear to be subject to large random moments. Nevertheless the results are consistent with a primary magnetization in the direction of the stable groups, with a variable

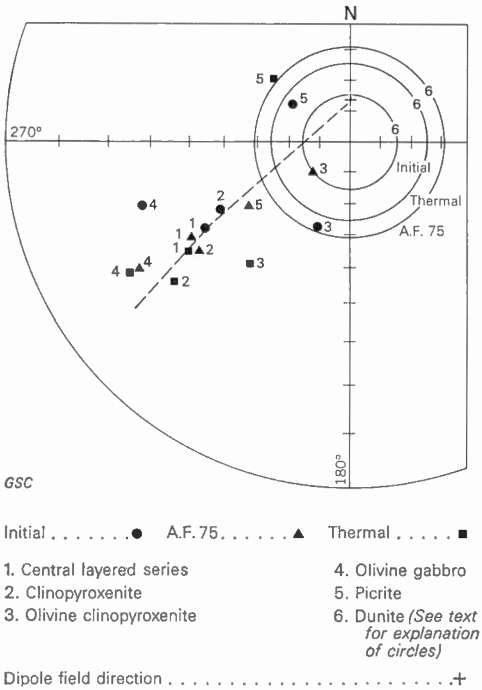

FIGURE 10. Stereographic projection showing the effect of cleaning the olivine-bearing rocks compared with the whole central layered series. The dipole field direction and great circle joining it to the mean directions for the central layered series are shown.

IRM superposed. The IRM is partly removed by cleaning, yielding directions that tend towards those of the stable groups. More severe treatment might take the process further, as suggested by analogy with the results from the Great Dyke (McElhinney and Gough, 1963). A tentative conclusion is that there is no later CRM (type 3), because any CRM in the altered rocks appears to be in the same direction as the TRM of the unaltered rocks (i.e., type 1); also the altered rocks have acquired secondary viscous components (type 4), and this secondary veneer is partly resistant to the low grade cleaning it has received. Thus these palaeomagnetic results tend to favour an origin for the serpentinization penecontemporaneous with the cooling of the intrusion.

RESULTS

Directions of magnetization have been obtained for all sites before treatment, after magnetic cleaning in an alternating magnetic field of peak value 75 oe, and after *thermal cleaning,* mostly to 300°C. Results are given in Tables IV, V, and VI and Figures 11, 12, and 13. From these directions statistics (Fisher, 1953) and palaeomagnetic pole positions (Creer, Irving, and Runcorn, 1957) have been computed.

The directions have been computed on the assumption that the present attitude of the rocks is that in which they cooled. The layers of the central layered series of the Muskox Intrusion, which are thought to have accumulated horizontally, now dip to the north at angles ranging from 0 to 5 degrees. This is similar to the tilt of the overlying beds of the Hornby Bay Group from which we infer that the intrusion has undergone a similar small tilt to the north. The average dip of the layered series, computed from the three boreholes DDHS, DDHN, and DDHE (Fig. 2), is $3\frac{1}{2} \pm 1$ degrees (Findlay, D. C., pers. com.) which is no more than the probable orientation errors and has been disregarded.

The western part of the intrusion has an apparent displacement of about 5 miles to the south along a northerly trending shear (Fig. 2). Mean directions of magnetization have been computed from the most stable sites on each side of the shear and are given in Table V. The difference between these directions is not significant. The inference is that the dominant motion on the shear was one of translation with insignificant rotation, and that the rocks to the west of the shear are in the same relative attitude as those to the east.

The results from the Muskox complex have been divided into petrological groups based on the detailed field work and petrological studies of members of the Geological Survey of Canada (Smith, 1962; Findlay and Smith, 1965). The lavas and dykes are not divisible into groups on present data and each has been treated as a single group. Table V gives the results from each group using data from all sites combined in three ways: (1) each site is given unit weight in the B statistics; (2) each sample is given unit weight in the C statistics; (3) each site pole is given unit weight in calculating the group poles in the D statistics. The smaller circle of confidence (α) in the C statistics is due to the larger population, since two samples were taken from most sites. It may not always be valid to consider individual samples from one site as completely independent, and the more conservative error circles, using sites as units, are used in the final analysis. The C statistics using samples as units, however, give results directly comparable with much published work (Irving, 1964), although much early work quotes confidence limits using specimens as units.

Wide initial scatter for some groups is greatly reduced by both *magnetic* and *thermal cleaning* (e.g. Fig. 14). One of the treatments is effective for other groups (e.g., magnetic cleaning for picrite and heating for the peridotite layer, Table V).

The angle between the sample directions from about one-quarter of the sites is so large that the mean is clearly a poor estimate of the original field direction. Where more than two samples were collected Watson's (1956) test of randomness gives a criterion for rejecting meaningless site directions. Where only two samples were collected, those sites in which the resultant of the two unit vectors was less than 1.75 (for which the angular separation between the two vectors is more than one radian), have been discarded in the compilation of valid sites (Table VI).

The groups into which the Muskox complex has been divided are petrological and not chronological, and hence are related to the minerals present. The palaeomagnetic stability depends predominantly on the composition and texture of the magnetic minerals. Thus the stability characteristics due to composition should be similar within a group, and stability variations from site to site are likely to be due either to secondary alteration or to textural differences. Each group is made up of

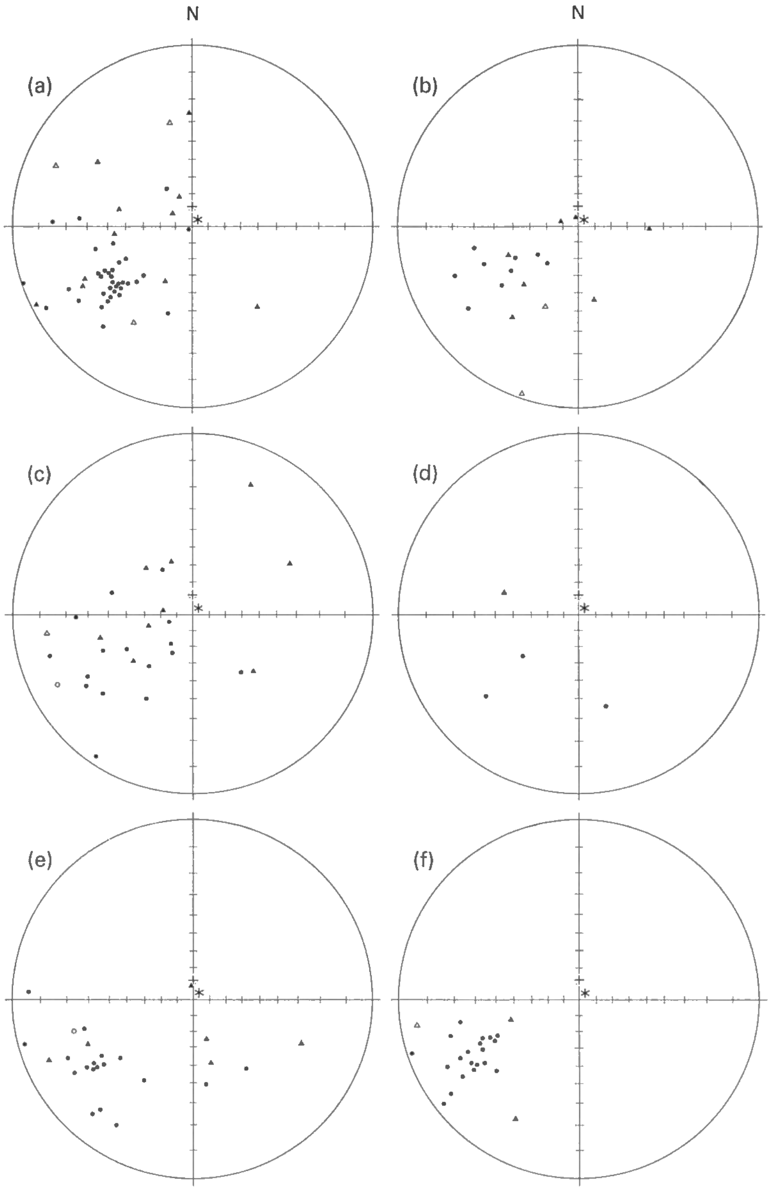

Mean site directions, angular dispersion, with N=2, R > 1.75 . . . . •
Mean site directions, angular dispersion, with N=2, R < 1.75 . . . . ▴
Field directions; dipole, present . . . . +, *

North seeking directions are plotted as open symbols on the upper hemisphere, and solid symbols on the lower hemisphere GSC

FIGURE 11. Stereographic projections, in which the primitive is the horizontal at each site, showing initial mean site directions for each group: (a) is the central layered series, (b) is the upper border zone, (c) is the marginal zone, (d) is baked contacts, (e) is the Mackenzie dyke swarm, and (f) is the Coppermine lava flows.

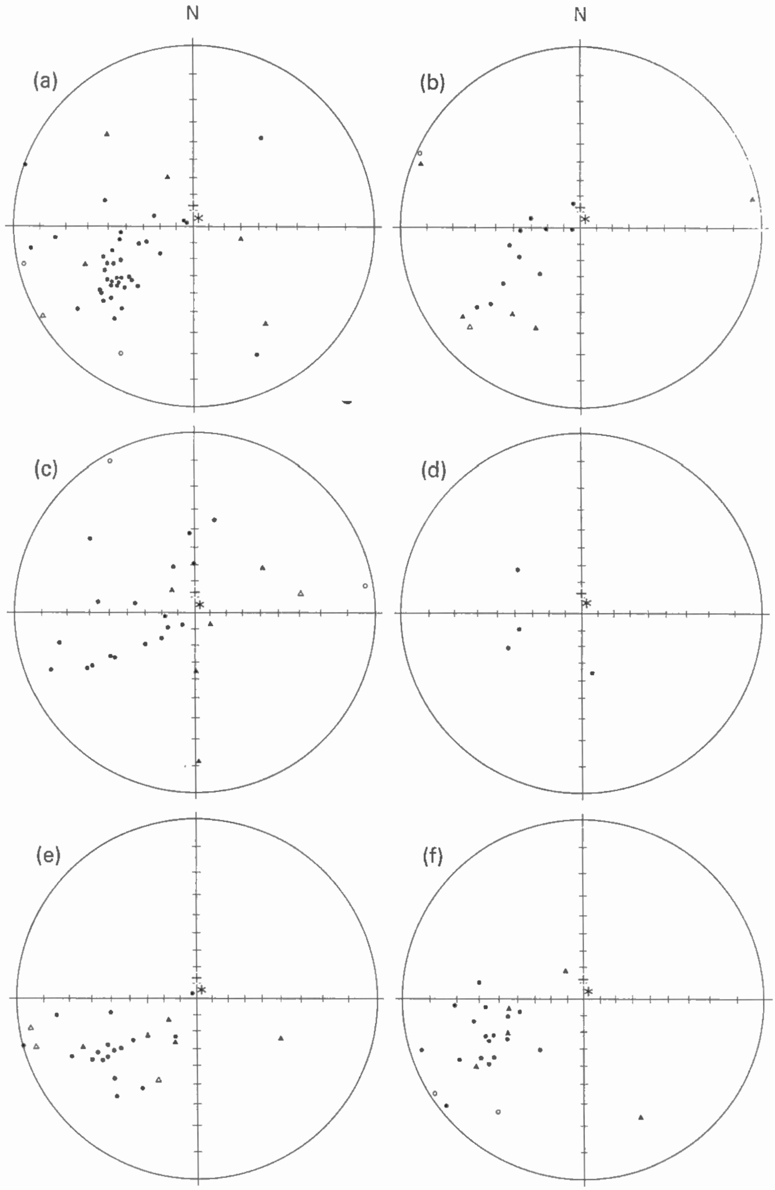

Mean site directions, angular dispersion, with N=2, R >1.75 . . . . •

Mean site directions, angular dispersion, with N=2, R < 1.75 . . . . ▲

Field directions; dipole, present . . . . +, *

North seeking directions are plotted as open symbols on the upper hemisphere, and solid symbols on the lower hemisphere

GSC

FIGURE 12. Mean directions from sites in groups as in Figure 11, after the specimens have been magnetically cleaned in an alternating magnetic field of 75 oe peak value.

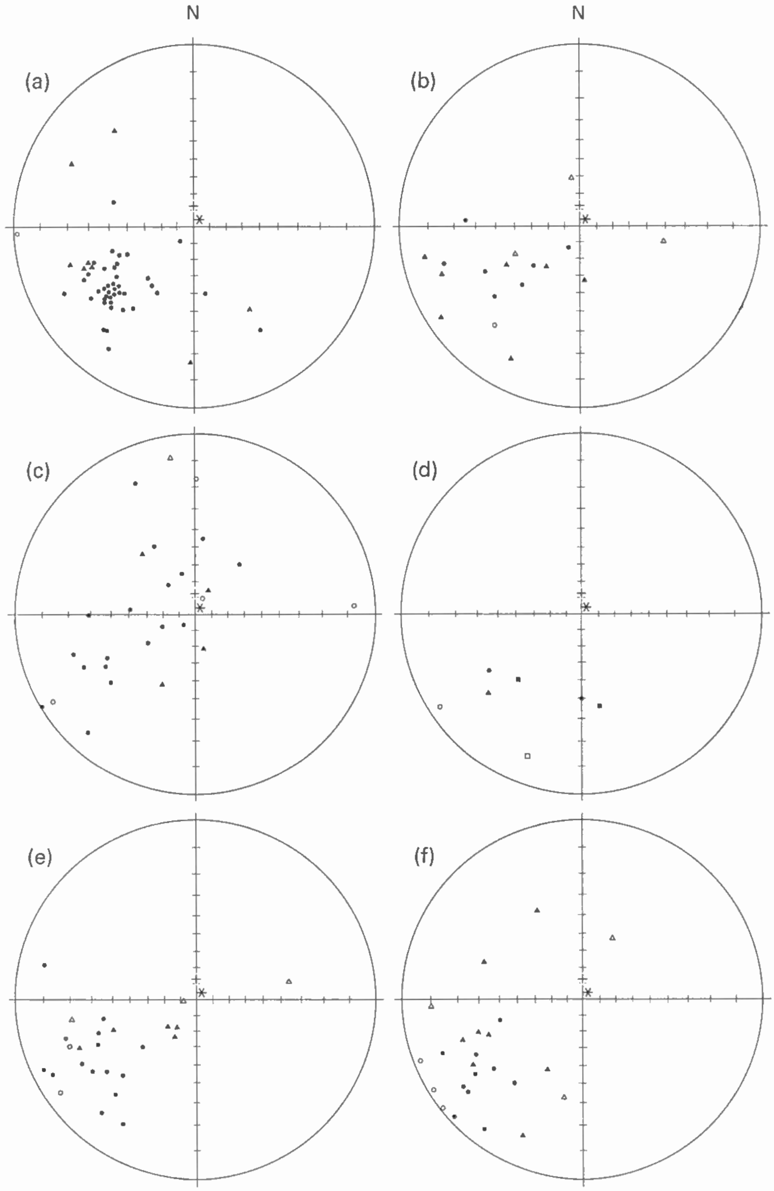

Mean site directions, angular dispersion, with N=2, R >1.75 . . . . •

Mean site directions, angular dispersion, with N=2, R <1.75 . . . . ▲

Field directions; dipole, present . . . . +, ✳

North seeking directions are plotted as open symbols on the upper hemisphere, and solid symbols on the lower hemisphere

In (d) the standard symbols are used after heating to 200°C., and ■ or □ represents directions after heating to 300°C.

GSC

FIGURE 13. Mean directions from sites in groups as in Figure 11 after thermal cleaning.

TABLE IV | *Site Statistics*

Site	Initial				A.F. 75				Heated				
	D	I	N	R	D	I	N	R	C°	D	I	N	R
	GRANOPHYRE 26 AND 27												
26A	342	+76	2	1.986	248	+31	2	1.760	210	177	+57	2	1.379
26B	262	+69	2	1.985	346	+85	2	1.728	210	231	+53	2	1.884
26C	242	+58	2	1.951	233	+60	2	1.990	210	226	+41	2	1.980
26D	227	−10	2	0.898	167	−45	2	1.593	210	249	−47	2	0.980
26E	217	+26	1	1.000	215	+26	1	1.000	210	222	+58	1	1.000
26F	231	+18	2	1.992	233	+16	2	1.995	210	221	−18	2	1.818
26G	243	+83	2	1.997	216	+60	2	1.972	210	213	+75	2	1.958
27A	203	+26	1	1.000	198	− 1	1	1.000	210	243	−41	1	1.000
27B	291	+ 3	2	1.201	93	+48	2	1.018	210	347	−60	2	1.566
27C	82	+ 2	2	0.931	202	−39	2	1.067	210	101	−41	1	1.000
27D	219	+51	2	1.997	236	+42	2	1.989	210	208	+11	2	1.896
	GRANOPHYRIC GABBRO 25												
25A	254	+46	2	1.914	242	+48	2	1.925	300	273	+24	2	1.833
25B	265	+53	2	1.060	277	+79	2	0.999	300	255	+14	2	1.832
25C	232	+11	1	1.000	222	+42	1	1.000	300	237	+ 5	1	1.000
25D	294	− 1	2	1.800	248	+17	2	1.952	300	251	+12	2	1.207
25E	228	+24	2	1.907	258	+29	2	1.944	300	245	+30	2	1.970
25F	233	+34	2	1.995	232	+34	2	1.988	300	231	+27	2	1.998
25G	278	+59	2	1.589	246	+44	2	1.630	300	259	+ 8	2	1.487
	GRANOPHYRE-BEARING GABBRO 24												
24A	250	+35	2	1.999	241	+34	2	1.991	300	237	+24	2	1.999
24B	285	+36	2	1.892	264	+44	2	1.696	300	287	+40	2	1.904
24C	250	+54	2	1.992	257	+32	2	1.803	300	238	+36	2	1.989
24D	106	+58	2	1.308	358	+26	2	1.146	300	172	+49	2	1.841
24E	280	+65	2	1.818	244	+41	2	1.972	300	183	+16	2	1.581
24F	331	+57	2	1.710	282	+45	2	1.661	300	228	+76	2	1.964
24H	238	− 2	2	1.542	241	+ 5	2	1.778	300	246	+32	2	1.975
24J	227	+40	2	1.964	272	+15	2	1.943	300	245	+21	2	1.831
24K	247	+59	2	1.993	227	+32	2	1.911	300	249	+42	2	1.846
24L	290	+ 1	2	1.145	294	−12	2	1.243	300	297	+16	2	1.325
	UPPER GABBRO 22a												
22aE	236	+31	2	1.993	229	+27	2	1.992	320	221	+27	2	1.999
22aF	245	+34	2	1.974	242	+30	2	1.989	320	246	+24	1	1.000
22aG	232	+37	2	1.999	232	+36	2	1.993	320	229	+32	2	1.991
	LOWER GABBRO 22b												
22bA	234	+13	2	1.999	236	+16	2	1.999	310	236	+16	2	1.998
22bB	228	+27	2	1.859	223	+48	2	2.000	310	223	+48	2	2.000
22bC	233	+31	2	1.997	231	+32	2	1.995	310	231	+33	2	1.993
22bD	228	+35	2	1.999	229	+35	2	1.997	310	229	+33	2	1.999

TABLE IV | *Site Statistics (cont.)*

Site	Initial				A.F. 75				Heated				
	D	I	N	R	D	I	N	R	C°	D	I	N	R
OLIVINE GABBRO 20													
20A	223	+40	2	1.817	206	+53	2	1.594	300	221	+16	2	1.943
20B	257	− 2	3	2.926	251	+ 0	3	2.952	300	268	− 1	3	2.710
20C	258	+45	2	1.951	241	+21	1	1.000	300	254	+39	2	1.860
20D	316	+21	2	1.200	336	+71	2	1.715	300	320	+22	2	1.351
20E	264	+16	2	1.966	243	+ 2	2	1.570	300	216	+11	2	1.932
PICRITIC WEBSTERITE 19													
19A	252	+39	2	1.971	241	+37	2	2.000	310	245	+39	2	1.996
19B	242	+32	2	1.985	229	+29	2	1.997	310	232	+28	2	1.995
19C	235	+35	2	1.988	242	+30	2	1.996	310	233	+32	2	1.969
19D	231	+34	3	2.943	234	+27	3	2.995	310	230	+25	1	1.000
19E	242	+37	2	1.942	230	+33	2	1.979	310	232	+29	2	1.974
WEBSTERITE 17													
17A	229	+24	2	1.999	228	+23	2	1.998	480	226	+25	2	1.985
17B	209	−11	2	1.976	210	−26	2	1.324	480	235	+33	2	1.941
17C	262	+ 6	2	1.932	243	+15	2	1.999	480	243	+12	2	1.992
17D	231	+32	2	1.976	228	+39	2	1.973	480	236	+30	2	1.981
17E	230	+40	2	1.987	231	+38	2	1.992	480	217	+47	2	1.986
18F	233	+35	2	1.993	233	+31	2	1.993	480	233	+27	2	1.998
17G	235	+35	2	1.998	234	+33	2	2.000	480	231	+30	2	1.998
18H	264	+46	2	1.975	243	+33	2	1.993	480	251	+29	2	1.946
OLIVINE CLINOPYROXENITE 16a													
16aA	228	+63	2	1.942	304	+26	2	1.344	310	244	+38	2	1.935
16aB	220	+28	2	1.988	326	+63	2	1.993	310	210	+45	2	1.748
16aC	285	+84	2	1.858	348	−31	2	1.654	310	248	+46	2	1.962
16aD	154	+13	2	1.979	195	+37	2	1.811	310	147	+22	2	1.997
16aE	144	+21	2	0.713	141	+29	2	0.759	310	147	+32	2	0.830
16aF	280	+85	2	1.947	229	+88	2	1.949	310	232	+26	2	1.983
CLINOPYROXENITE 16b													
16bA	38	+27	2	1.808	224	+43	2	1.970	310	218	+31	2	1.980
16bB	220	+22	2	2.000	222	+18	2	1.999	310	221	+16	2	2.000
16bC	234	+33	2	1.995	239	+35	2	1.992	310	230	+26	2	1.998
16bD	243	+41	2	1.873	244	+46	2	1.778	310	236	+20	2	1.999
16bF	249	+25	1	1.000	243	+23	1	1.000	310	250	+24	1	1.000
PERIDOTITE LAYER 12 AND 13													
13B	252	+26	2	1.956	258	+43	2	1.770	310	253	+19	1	1.000
13C	225	+16	2	1.978	273	+26	2	1.976	310	250	+28	1	1.000
13J	262	+44	1	1.000	303	+76	1	1.000	310	250	+28	1	1.000
PERIDOTITE MARGIN 12 AND 13													
13A	312	+71	2	1.160	253	+62	2	0.545	310	167	+67	2	1.127
13D	278	+53	2	1.995	285	+40	2	1.906	310	275	+51	2	1.996

TABLE IV | *Site Statistics (cont.)*

Site	Initial				A.F. 75				Heated				
	D	I	N	R	D	I	N	R	C°	D	I	N	R
13E	131	+77	2	1.526	274	+72	2	1.390	310	30	+73	2	1.901
13F	247	+ 9	2	1.962	243	− 9	2	1.976	310	238	− 5	2	1.987
13G	241	+60	2	1.963	255	+36	2	1.706	310	239	+31	2	1.752
13H	305	+20	2	1.824	315	+51	2	1.095	310	351	− 8	1	1.000
13K	240	+34	2	1.985	236	+20	2	1.979	310	221	+ 8	2	1.801
12A	242	+25	2	1.984	223	− 3	2	1.989	310	204	+44	2	0.638
12B	12	+35	2	1.981	231	+45	2	1.505	310	6	+45	2	1.961
	PICRITE MARGIN 15												
15A	57	+41	2	1.546	64	+28	2	1.527	320	319	+43	2	1.054
15B	237	+70	2	1.937	218	+48	2	1.832	320	239	+56	2	1.898
15C	236	+52	2	1.945	247	+34	2	1.997	320	243	+33	2	1.992
15D	330	− 3	2	1.966	338	+55	2	1.741	320	0	−17	2	1.930
15E	80	−28	5	0.964	140	+44	2	3.896	320	231	+28	2	1.985
15F	178	+52	2	1.297	25	+18	2	0.547	320	317	+65	2	1.888
15G	81	− 3	2	1.895	132	+39	2	1.100	320	87	− 8	2	1.912
15H	178	+ 8	1	1.000	208	+34	2	1.920	320	335	+13	2	1.993
15J	2	+61	2	1.905	262	−12	2	0.977	320	41	+50	2	1.895
15K	358	+43	2	1.753	214	+67	2	1.984	320	340	+64	2	1.935
15L	256	+72	2	1.909	206	+63	2	1.975	320	249	+68	2	1.940
15M	275	+34	2	1.988	268	+26	2	1.992	320	269	+29	2	1.994
15N	239	+36	2	1.894	228	+23	2	1.968	320	23	−80	2	1.970
15P	335	+60	2	1.973	325	+57	2	1.965	320	329	+43	2	1.870
15Q	219	+78	2	1.991	245	+75	2	1.969	320	228	+79	2	1.984
	NORITE MARGIN 21												
21C	230	+64	9	8.041	242	+46	8	7.221	300	230	− 0	9	6.207
21J	257	+16	3	2.883	253	+12	2	1.938	300	252	+20	2	1.983
21K	242	+23	2	1.999	238	+22	2	1.999	300	245	+22	2	1.996
	BAKED CONTACTS 30												
30A	243	+41	2	1.948	285	+44	2	1.472	210	201	−10	2	1.551
30B	302	+45	2	1.812	228	+22	2	1.993	210	168	+35	2	1.209
30B									310	230	+22	1	1.000
30C	253	+50	3	2.852	233	+47	3	2.844	210	224	+37	3	1.528
30C									310	239	+28	2	1.988
30E	170	+51	4	3.489	163	+33	4	2.850	210	148	+59	4	3.132
30E									310	180	+40	4	2.789
30F									310	237	− 4	2	1.791
	DYKES												
29A	236	+38	2	1.994	237	+24	2	2.000	300	253	+17	2	1.989
29C	236	+28	2	1.998	237	+21	2	1.995	300	240	+19	2	1.972
29D	219	+21	2	1.964	220	+13	2	1.758	300	220	+21	2	1.991
29E	245	+16	2	1.996	245	+16	2	1.995	300	245	+15	2	1.993
29F	239	+23	2	2.000	235	+24	2	2.000	300	235	+21	2	1.997

TABLE IV | *Site Statistics (conc.)*

Site	Initial				A.F. 75				Heated				
	D	I	N	R	D	I	N	R	C°	D	I	N	R
29G	237	+34	2	1.994	247	+26	1	1.000	300	245	+29	2	1.960
29H	236	+45	5	4.483	234	+27	5	4.813	300	242	+ 7	2	1.999
29J	273	+15	2	1.984	273	+ 6	2	1.992	300	283	+ 9	2	1.991
29K	260	+39	2	1.986	255	+26	2	1.994	300	258	+35	2	1.985
29L	229	+68	2	1.369	199	+64	2	1.454	300	213	+69	2	1.493
29M	253	− 5	2	1.449	247	+ 9	2	1.020	300	269	−82	2	1.679
29N	210	+30	2	1.945	188	+39	2	1.889	300	210	+13	2	1.980
29P	204	−37	2	1.543	149	−12	2	1.907	300	79	−35	2	1.464
29Q	115	+35	2	1.040	112	+24	2	1.670	300	250	+39	2	1.728
29R	236	+29	2	1.999	235	+23	2	1.990	300	231	+25	2	1.993
29S	255	0	2	1.778	255	−22	2	1.890	300	249	−17	2	1.855
29T	207	+63	2	1.750	196	+50	2	1.634	300	224	+30	2	1.935
29U	338	+87	2	1.987	238	+75	2	1.837	300	227	+47	2	1.829
29V	242	+33	2	1.987	231	+36	2	1.927	300	251	+31	2	1.989
29W	241	+27	2	1.989	238	+29	2	1.976	300	247	+21	1	1.000
29X	260	− 5	2	1.824	255	+ 3	2	1.959	300	261	−21	1	1.000
29Y	231	+53	2	1.297	359	+81	2	1.459	300	209	+64	2	0.911
29Z	205	+61	2	1.500	142	+39	2	1.934	300	225	+66	2	1.457
29AA	225	+25	2	1.973	211	+35	2	1.881	300	220	+12	2	1.950
29BB	247	+22	2	1.861	221	+10	2	1.987	300	235	− 6	2	1.912
	LAVA FLOWS 10				In Order of Age, Youngest at Top								
10J	279	+30	2	1.878	258	+23	2	1.990	480	231	+11	2	1.847
10K	235	+25	2	1.993	236	+20	2	1.997	480	235	+18	2	1.992
10L	154	+17	2	1.738	207	+16	2	1.680	480	204	+11	2	1.737
10M	217	−13	2	1.792	233	+ 7	2	1.930	480	251	+20	2	0.980
10N	221	+49	2	1.937	228	+27	2	1.997	480	256	+40	2	1.769
10R	245	+41	2	1.692	244	+21	2	1.894	480	219	+28	2	1.186
10Q	237	− 1	2	1.968	243	+17	2	1.933	480	228	+ 2	2	1.975
10P	252	+ 4	2	1.988	251	+ 2	2	1.991	480	249	− 2	2	1.998
10H	244	+15	2	1.964	237	+22	2	1.982	480	247	+28	2	1.886
10G	232	+ 2	2	1.994	232	+ 3	2	1.993	480	232	− 1	2	1.991
10F	241	+39	2	1.888	246	+31	2	1.933	480	268	−10	2	1.741
10E	248	+31	2	1.978	245	+28	2	1.997	480	243	+22	2	1.944
10D	261	+45	2	1.735	252	+46	2	1.723	480	333	+32	2	0.265
10C	257	+27	2	1.920	246	+34	2	1.998	480	191	−32	2	1.341
10B	236	−20	2	1.358	260	− 5	2	1.583	480	238	− 2	2	1.913
10A	256	+44	2	1.999	245	+37	2	1.994	480	205	+43	2	1.685
10W	266	+20	2	1.826	253	+17	2	1.942	480	249	+10	2	1.980
10V	326	+71	2	0.654	236	+14	2	2.000	480	26	−48	2	0.159
10U	257	+51	2	1.799	243	+36	2	1.982	480	291	+30	2	1.310
10T	240	+24	2	1.990	238	+21	2	1.977	480	238	+20	1	1.000
10S	265	+34	2	1.900	242	+28	2	1.978	480	217	+ 6	2	1.908
10X	246	+31	2	1.971	242	+11	2	1.995	480	234	+11	2	1.979
10Y	236	+29	2	1.993	235	+25	2	1.996	480	232	+26	2	1.996
10Z	248	+34	5	4.727	270	+42	2	1.909	480	249	+32	1	1.000

TABLE V Group Statistics using all Samples and Sites

Group	B Statistics Sites Unit Weight										C Statistics Samples Unit Weight										D Statistics Poles Unit Weight						Treatment
	D_l	I_l	N_l	R_l	k_l	α_l	Lat.	dp	Long.	dm	D_s	I_s	N_s	R_s	k_s	α_s	Lat.	dp	Long.	dm	Lat.	Long.	N_p	R_p	k_p	α_p	
26 and 27	232	+50	11	7.329	2.7	34	15N	31	159W	46	236	+55	20	12.631	2.6	26	21N	26	161W	37	23N	159W	11	7.137	2.6	36	Initial
Granophyre	212	+34	11	7.224	2.6	35	1S	23	145W	40	218	+38	20	11.916	2.4	28	3N	19	150W	33	4N	144W	11	7.587	2.9	33	A.F. 75
	220	+12	11	5.186	1.7	53	12S	27	155W	53	220	+21	19	8.765	1.8	38	7S	21	155W	40	8S	155W	11	6.333	2.1	42	Th. 210°C
25	253	+35	7	6.139	7.0	25	11N	16	178E	28	253	+35	13	9.880	3.8	24	11N	16	177E	28	13N	178E	7	6.289	8.4	22	Initial
Granophyric	243	+43	7	6.569	14	17	13N	13	171W	21	244	+39	13	10.860	5.6	19	11N	14	173W	23	16N	171W	7	6.506	12	18	A.F. 75
gabbro	250	+17	7	6.761	25	12	1N	7	177E	13	251	+19	13	10.932	5.8	19	2N	10	177E	20	1N	177E	7	6.808	31	11	Th. 300°C
24	262	+50	10	7.952	4.4	26	25N	23	175E	35	260	+50	20	14.375	3.4	21	24N	19	177E	28	29N	177E	10	7.430	3.5	30	Initial
Granophyre-	265	+31	10	8.221	5.1	24	14N	15	166E	27	260	+31	20	14.686	3.6	20	12N	13	170E	23	14N	167E	10	8.271	5.2	23	A.F. 75
bearing-gabbro	241	+41	10	8.330	5.4	23	11N	17	170W	28	240	+41	20	15.464	4.2	18	11N	14	169E	22	13N	168W	10	8.026	4.6	26	Th. 300°C
22a	238	+34	3	2.988	172	10	5N	6	169W	11	238	+34	6	5.943	87	7	5N	5	169W	8	6N	169W	3	2.987	151	10	Initial
Upper	234	+31	3	2.983	114	12	3N	7	166W	13	234	+31	6	5.939	82	7	3N	5	166W	8	3N	166W	3	2.984	127	11	A.F. 75
gabbro	232	+28	3	2.955	45	19	0N	11	165W	20	229	+29	5	4.932	59	10	0S	6	162W	11	0N	165W	3	2.951	41	20	Th. 320°C
22b	231	+26	4	3.957	69	11	1S	7	164W	12	231	+26	8	7.767	30	10	1S	6	164W	11	1S	163W	4	3.983	175	7	Initial
Lower	230	+33	4	3.913	35	16	2N	10	162W	18	230	+33	8	7.817	38	9	2N	6	162W	10	3N	162W	4	3.955	67	11	A.F. 75
gabbro	230	+33	4	3.911	34	16	2N	10	162W	18	230	+33	8	7.812	37	9	2N	6	162W	11	3N	162W	4	3.955	66	11	Th. 310°C
20	265	+27	5	4.268	5.5	36	11N	21	166E	39	260	+23	11	8.608	4.2	26	7N	14	169E	27	12N	167E	5	4.319	5.9	35	Initial
Olivine	244	+32	5	4.011	4.0	44	7N	28	175W	49	247	+28	10	7.016	3.0	34	5N	20	178W	37	13N	174W	5	3.950	3.8	45	A.F. 75
gabbro	254	+22	5	3.969	3.9	45	4N	25	175W	47	251	+19	11	8.047	3.4	29	2N	16	176E	30	5N	174E	5	3.982	3.9	44	Th. 300°C
19	240	+36	5	4.970	132	7	7N	4	171W	8	239	+36	11	10.760	42	7.2	7N	5	170W	8	7N	171W	5	4.963	109	7	Initial
Picritic	235	+31	5	4.975	161	6	3N	4	167W	7	235	+31	11	10.914	116	4.3	3N	3	167W	5	3N	167W	5	4.976	166	6	A.F. 75
Websterite	234	+30	5	4.969	127	7	2N	4	166W	8	235	+31	9	8.879	66	6.4	3N	4	167W	7	3N	166W	5	4.974	152	6	Th. 310°C
17	236	+27	8	7.351	11	18	1N	11	168W	19	236	+27	16	14.560	10	12	1N	7	168W	13	2N	168W	8	7.564	16	14	Initial
Websterite	231	+24	8	7.437	12	16	2S	9	165W	17	232	+26	16	14.442	9.6	13	1S	7	165W	14	2S	165W	8	7.745	28	11	A.F. 75
	234	+29	8	7.822	39	9	2N	5	167W	10	234	+29	16	15.475	29	7	2N	4	167W	8	2N	166W	8	7.858	49	8	Th. 480°C
16b	242	+44	5	3.518	2.7	58	14N	45	170W	73	240	+46	9	6.020	2.7	39	14N	32	168W	50	14N	170W	5	3.162	2.2	69	Initial
Clino-	234	+33	5	4.855	28	15	4N	10	165W	17	233	+34	9	8.486	16	14	4N	9	164W	15	5N	165W	5	4.896	39	13	A.F. 75
pyroxenite	231	+24	5	4.899	39	12	2S	7	165W	13	229	+24	9	8.823	45	7.7	3S	4	163W	8	3S	165W	5	4.900	40	12	Th. 310°C
16a	183	+57	6	4.691	3.8	40	14N	42	117W	57	192	+59	12	8.284	3.0	31	18N	35	125W	46	26N	123W	6	4.305	2.9	47	Initial
Olivine-clino-	285	+73	6	3.041	1.7	78	57N	124	177E	139	295	+68	12	5.316	1.6	53	55N	74	161E	88	61N	179W	6	2.549	1.4	—	A.F. 75
pyroxenite	204	+44	6	4.920	4.6	35	4N	27	137W	44	211	+43	12	8.690	3.3	28	5N	22	143W	35	5N	138W	6	4.619	3.6	41	Th. 310°C

13e	245	+29	3	2.856	14	34	5N	20	176W	38	241	+26	5	4.720	14	21	5N	12	176W	23	6N	177W	3	2.876	16	32	Initial
Peridotite	270	+49	3	2.767	8.6	45	27N	39	167E	60	269	+43	5	4.445	7.2	31	22N	24	166E	38	33N	168E	3	2.719	7.1	50	A.F. 75
layer	251	+25	3	2.991	223	8	5N	5	177E	9	251	+25	3	2.991	223	8	5N	5	177E	9	5N	177E	3	2.996	566	5	Th. 320°C
12 and 13	278	+52	9	7.089	4.2	29	33N	28	162E	40	276	+50	18	12.892	3.3	23	30N	21	163E	31	37N	162E	9	6.554	3.3	34	Initial
Peridotite	252	+38	9	7.536	5.5	24	13N	17	180	28	249	+32	18	11.796	2.7	26	8N	16	179W	29	17N	179E	9	7.721	6.3	22	A.F. 75
margin	256	+55	9	5.446	2.3	45	28N	45	177W	64	258	+53	17	8.848	2.0	36	26N	35	179E	51	35N	172W	9	4.646	1.8	55	Th. 320°C
15	301	+83	15	8.311	2.1	36	70N	69	155W	70	303	+77	32	15.885	1.9	26	68N	46	177E	49	66N	158W	15	6.478	1.6	47	Initial
Picrite	236	+68	15	9.739	2.7	29	35N	41	155W	49	223	+66	33	19.577	2.4	21	29N	28	147W	34	37N	153W	15	7.801	1.9	39	A.F. 75
	310	+57	15	8.327	2.1	36	49N	38	134E	52	308	+57	30	15.277	2.0	27	49N	28	136E	39	51N	138E	15	7.593	1.9	40	Th. 320°C
21	246	+34	3	2.762	8.4	46	9N	30	176W	52	242	+48	14	11.845	6.0	18	17N	15	169W	23	11N	176W	3	2.823	11	39	Initial
Norite	245	+27	3	2.891	18	30	4N	17	177W	32	244	+36	12	10.790	9.1	15	9N	10	173W	18	4N	176W	3	2.945	36	21	A.F. 75
	246	+14	3	2.941	34	22	3S	11	180W	22	243	+ 8	13	9.976	4.0	24	7S	12	178W	24	3S	180W	3	2.974	78	14	Th. 300°C
30	237	+50	5	4.688	13	22	17N	20	164W	30	231	+53	13	11.199	6.7	17	17N	17	158W	24	17N	163W	5	4.466	7.5	30	Initial
Baked	224	+40	5	4.259	5.4	36	5N	26	155W	44	217	+41	13	9.269	3.2	28	4N	20	149W	33	7N	156W	5	4.060	4.3	42	A.F. 75
contacts	202	+27	5	3.954	3.8	45	7S	27	136W	49	198	+33	13	7.080	2.0	40	4S	26	132W	46	5S	133W	5	4.103	4.5	41	Th. 210°C
	224	+23	4	3.589	7.3	37	5S	21	158W	39	219	+27	9	6.621	3.4	33	4S	20	153W	36	4S	157W	4	3.634	8.2	34	Th. 310°C
10	244	+29	24	20.879	7.4	12	5N	7	176W	13	244	+28	51	41.730	5.4	10	4N	6	176W	10	6N	177W	24	21.285	8.5	11	Initial
Lava	242	+22	24	22.998	23	6	1N	4	176W	7	242	+22	48	44.559	14	6	1N	3	176W	6	1N	175W	24	23.317	34	5	A.F. 75
flows	240	+15	24	19.107	4.7	15	4S	8	176W	16	237	+14	46	33.615	3.6	13	5S	7	172W	13	3S	176W	24	19.464	5.1	15	Th. 480°C
29	236	+33	26	28.827	6.0	13	4N	8	167W	14	237	+33	55	43.072	4.5	10	5N	7	168W	12	7N	165W	26	22.152	6.5	12	Initial
Dykes	227	+31	26	20.270	4.4	15	1N	10	160W	17	228	+30	54	39.745	3.7	12	0N	7	160W	13	4N	158W	26	20.090	4.2	16	A.F. 75
	239	+21	25	19.228	4.2	16	1S	9	172W	17	239	+20	48	35.065	3.6	13	2S	7	173W	13	1S	171W	25	20.247	5.0	14	Th. 300°C
9											60	+24	6	4.774	4.1	38	23N	22	2W	40							Initial
Sill											65	+15	6	5.453	7.6	26	17N	14	5W	27							A.F. 150
											72	+ 6	6	5.603	13	20	10N	10	10W	20							A.F. 300
											83	−23	6	4.601	3.6	41	8S	23	14W	44							Th. 480°C
8											237	+37	1				7N	—	168W	—							Initial
Intercalated											236	+24	1				1S	—	170W	—							A.F. 150
sandstone											272	+26	1				13N	—	158E	—							Th. 210°C
Fault rotation test																											
West side	238	+34	9	8.739	31	9	5N	6	168W	11																	A.F. 75
East side	235	+31	12	11.698	36	7	3N	5	166W	8																	A.F. 75

D is the declination measured east of true north. I is the inclination positive downwards. N is the number of unit vectors. R is the resultant length of the vector addition of the unit vectors. k is Fisher's estimate of precision. α is the half-angle of the cone of confidence at a probability of P = 0 .05. The subscript indicates that the data are compiled using sites as units. The subscript s indicates that the data are compiled using samples as units. The subscript p indicates that the data refer to a mean pole position calculated from the pole position of individual sites. A.F. is the peak value of the alternating magnetic field to which the specimens were subjected before measurement. Th. is the temperature to which the specimens were raised in zero magnetic field and oxygen-free atmosphere before measurement. dp and dm are the semi-axes of the oval of confidence about the pole position; dp lies along the palaeomeridian through the site position, dm is perpendicular to it. The number in the Group column refers to the petrological unit.

sites from different horizons in the body, so that field oscillations with periods of hundreds of years should be smoothed out in the group means.

The three major units, the upper border zone, the central layered series, and the marginal zone, have been separated in the statistical analysis and the results are shown in Table VII, together with results from the dykes and lavas. The upper border zone is heterogeneous and contains partly digested fragments of country rock. This variability appears to be reflected by dispersion in the magnetic results of the group (Table VI), but the mean zone directions after treatment agree well with those from the layered series. The marginal zone is affected both by lineation,

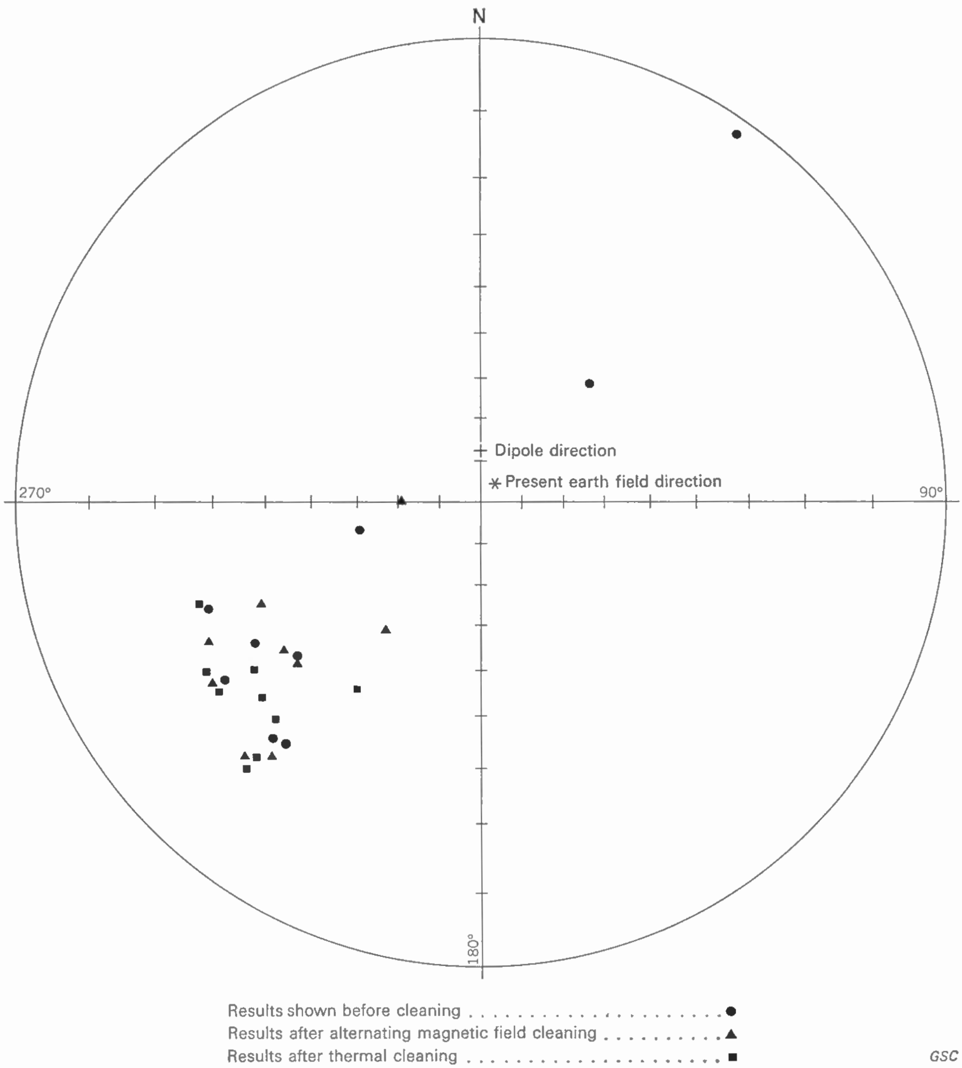

FIGURE 14. Stereographic projections showing the sample directions of clinopyroxenite group; directions shown are plotted on the lower hemisphere.

TABLE VI | *Group Statistics from Valid Sites*

Rock Number and Group	Treatment	D	I	N	R	k	α
UPPER BORDER ZONE							
26 and 27 Granophyre	Initial	241	+63	6	5.416	8.6	24
	A.F. 75	235	+42	5	4.749	16	20
	Thermal	220	+33	5	4.208	5.1	38
25 Granophyric gabbro	Initial	253	+29	4	3.487	5.8	42
	A.F. 75	245	+32	4	3.889	27	18
	Thermal	251	+24	4	3.865	22	20
CENTRAL LAYERED SERIES							
24 Granophyre-bearing-gabbro	Initial	255	+50	6	5.713	17	17
	A.F. 75	247	+27	6	5.709	17	17
	Thermal	241	+43	8	7.185	8.6	20
22a Upper gabbro	Initial	238	+34	3	2.988	171	10
	A.F. 75	234	+31	3	2.983	114	12
	Thermal	232	+28	3	2.955	45	19
22b Lower gabbro	Initial	231	+26	4	3.957	69	11
	A.F. 75	230	+33	4	3.913	35	16
	Thermal	230	+32	4	3.911	34	16
20 Olivine gabbro	Initial	252	+26	4	3.664	8.9	33
	A.F. 75	239	+19	4	3.620	7.9	35
	Thermal	239	+18	4	3.605	7.6	36
19 Picritic websterite	Initial	240	+36	5	4.970	132	7
	A.F. 75	235	+31	5	4.975	161	6
	Thermal	234	+30	5	4.969	127	7
17 Websterite	Initial	236	+27	8	7.351	11	18
	A.F. 75	235	+30	7	6.906	64	8
	Thermal	234	+29	8	7.822	39	9
16b Clinopyroxenite	Initial	242	+44	5	3.518	2.7	58
	A.F. 75	234	+33	5	4.855	28	15
	Thermal	231	+24	5	4.899	39	12
16a Olivine-clinopyroxenite	Initial	200	+61	5	4.052	4.2	42
	A.F. 75	229	+75	3	2.570	4.6	65
	Thermal	219	+41	4	3.279	4.2	51
13 Peridotite layer	Initial	245	+29	3	2.856	14	34
	A.F. 75	271	+49	3	2.767	8.6	45
	Thermal	251	+25	3	2.991	223	8
MARGINAL ZONE							
13m Peridotite margin	Initial	270	+42	7	5.513	4.0	34
	A.F. 75	244	+13	4	3.513	6.2	40
	Thermal	252	+45	4	3.069	3.2	61
15 Picrite	Initial	302	+68	11	7.707	3.0	32
	A.F. 75	237	+52	9	7.978	7.8	20
	Thermal	308	+59	14	7.365	2.0	40

TABLE VI | *Group Statistics from Valid Sites (conc.)*

Rock Number and Group	Treatment	D	I	N	R	k	α
MARGINAL ZONE (cont'd)							
	Initial	246	+34	3	2.762	8.4	46
21 Norite	A.F. 75	245	+27	3	2.892	18	30
	Thermal	246	+14	3	2.941	34	22
	Initial	246	+27	17	16.180	20	8
10 Lava flows	A.F. 75	243	+22	21	20.419	34	5
	Thermal	236	+11	12	11.662	33	8
	Initial	240	+31	20	18.373	12	10
29 Dykes	A.F. 75	230	+25	21	17.573	6	14
	Thermal	239	+19	17	15.781	13	10

D, I, N, R, k and α have the same meaning as for Table V, as do the numbers in the Rock Group column. The data are compiled using sites as units, and are thus comparable with the B Statistics of Table V.

a possible cause of magnetic anisotropy, and secondary alteration (*see* Laboratory Studies). Both the upper border zone and the marginal zone give less scattered directions that agree more nearly with those of the central layered series after *magnetic cleaning,* but not after *thermal cleaning.*

The central layered series is the least disturbed part of the intrusion, but the untreated NRM directions from the olivine-bearing group and some of the pyroxene groups are widely scattered (*see* Table IV). The scatter in the olivine-bearing groups remained high after both types of cleaning, but the mean directions tended towards those of the stable groups (Fig. 14), whereas the scatter in the stable groups increased slightly.

The small change in direction of the mean for the central layered series after both *thermal* and *magnetic cleaning* is away from the present earth's field direction, suggesting the removal of a small viscous secondary component directed along this field, and the increase in precision after *thermal cleaning* indicates that small randomly oriented secondary components were also removed.

All the petrological units of the Muskox Intrusion must have cooled in an instant of geological time, and both field evidence and radiogenic age determinations point to a similar age for the lavas and probably the dykes studied. The groups presented here display a wide range of chemical composition, from ultramafic to felsic, and cooled under a wide range of physical conditions, from atmospheric pressure for the extrusive rocks to high hydrostatic pressure for the lower layers of the Muskox Intrusion, and an unknown but probably wide range of directed stress. The good agreement between the treated direction of the lavas, the dykes, the country rock baked by the intrusion, and its three major units (Table VII), all of which are thought to have acquired their primary magnetization

TABLE VII | *Zone Statistics*

Major Units	B Statistics: Groups Unit Weight										C Statistics: Sites Unit Weight										D Stats: Group Poles Unit Weight						Treatment
	D	I	N	R	k	α	Lat.	dp	Long.	dm	D	I	N	R	k	α	Lat.	dp	Long.	dm	Lat.	Long.	N	R	k	α	
Upper border zone	249	+46	2	1.907	11	86	17.3N	70	175.3W	110	248	+50	10	8.507	6.0	21	19.9N	19	172.8W	29	19.4N	173.3W	2	1.928	14	73	None
	240	+37	2	1.988	81	28	8.5N	19	170.2W	33	240	+38	9	8.583	19	12	8.6N	8	169.6W	14	8.5N	170.0W	2	1.989	93	26	A.F. 75
	236	+30	2	1.936	16	68	2.5N	42	168.0W	76	235	+30	9	7.815	6.7	21	2.4N	13	167.3W	24	2.4N	167.5W	2	1.927	14	74	Thermal
Central layered series	239	+38	9	8.678	25	11	8.3N	7	169.1W	12	239	+38	43	37.673	7.9	8	8.3N	6	169.1W	10	9.2N	168.2W	9	8.660	24	11	None
	239	+37	9	8.574	19	12	7.8N	8	169.3W	14	238	+34	40	37.032	13	6	5.8N	4	169.3W	7	9.8N	168.8W	9	8.548	18	13	A.F. 75
	235	+30	9	8.853	54	7	2.4N	4	166.8W	8	235	+31	44	41.014	14	6	3.0N	4	166.8W	7	2.7N	166.6W	9	8.882	68	6	Thermal
Marginal zone	266	+50	3	2.827	12	38	26.4N	34	171.8E	51	274	+55	21	15.123	3.4	20	34.0N	21	167.1E	29	29.8N	170.4E	3	2.762	8.4	46	None
	242	+30	3	2.876	16	32	5.0N	20	173.7W	35	241	+38	16	13.730	6.6	16	8.9N	11	170.8W	18	6.1N	172.9W	3	2.940	33	22	A.F. 75
	261	+42	3	2.683	6.3	54	19.1N	41	172.7E	66	274	+50	21	11.970	2.2	29	29.7N	26	164.7E	38	22.8N	170.7E	3	2.660	5.9	56	Thermal
Lava flows											246	+27	17	16.180	20	8											None
											243	+22	21	20.419	34	5											A.F. 75
											236	+11	12	11.662	33	8											Thermal
Dykes											240	+31	20	18.373	12	10											None
											230	+25	21	17.573	6	14											A.F. 75
											239	+19	17	15.781	13	10											Thermal

in late Middle Proterozoic time, is strong evidence supporting the idea that the direction obtained is that of the earth's magnetic field at that time. The good grouping of the directions from over forty sites within the central layered series enables this direction to be calculated with considerable accuracy.

ANCIENT CYCLIC MAGNETIC FIELD CHANGES

The magnitude of the short period variations in the earth's magnetic field in remote epochs, comparable with those which cause secular variation in the recent field, is of geophysical interest not only as an aid in the interpretation of scatter of palaeomagnetic results, but also as a possible pointer to the evolution of the earth's magnetic field. Attempts have been made to use series of lava flows (Chevallier, 1925; Doell and Cox, 1963) or varves (Johnson, Murphy, and Torreson, 1948; Torreson, Murphy, and Graham, 1949; Granar, 1958; Griffiths, *et al.,* 1960) to determine *secular variation* from palaeomagnetic results from Tertiary and Quaternary rocks, and Jaeger and Green (1956) showed how the cooling of a thick intrusive sheet might be used to study short period field variations during cooling.

Two main obstacles arise in such a study using palaeomagnetic directions. The first is the difficulty of obtaining a valid time base to cover a few thousand years, and the second is the impracticability, enhanced in older rocks, of filtering out from the observations other variables of comparable or greater magnitude than the cyclic variations being studied.

Four groups of data were obtained from the Muskox Intrusion, which might give such information. Jaeger's (1957; 1958) work on the cooling of igneous bodies provides a time base for the traverse across the feeder (Fig. 2, site 21C) and vertically up the sill. Unfortunately the time span covered by the passage of the blocking temperature isotherm from the margin to the centre of the *feeder* is probably no more than 250 years (Jaeger and Green, 1956), and for the sill much less. No systematic pattern of direction change emerges from the directions across the *feeder* (Table VIII); any regular variation appears to be masked by irregularities. A fault close to the traverse line may have caused rotation of some samples, and it is also possible that secondary components are not eliminated in the cleaned directions. The thickness of the sill is not known, but fine-grained samples at the bottom (RN134) and top (RN139) are likely to be close to the margin. Based on this criterion 140 feet is a reasonable estimate of the thickness. Figure 15 shows the variation of *declination* (D) and *inclination* (I) with distance from the base of the sill. There is a suggestion of symmetry between the top and bottom of the sill for inclination, but those for declination appear to cover almost a complete cycle covering some 40 degrees of arc. A possible explanation of the D curve is that the top sample is in the middle of the sill, the top half having been removed by erosion. The changes in D (38°) and I (56°) are of the same order of magnitude as those from recent *secular variation* measurements. The use of only two specimens from each level allows the possibility of large fluctuation errors; to obtain reliable points for the curves it would be necessary to measure enough specimens at each level to get an estimate of the reliability of the mean value from a statistical analysis (Fisher, 1953).

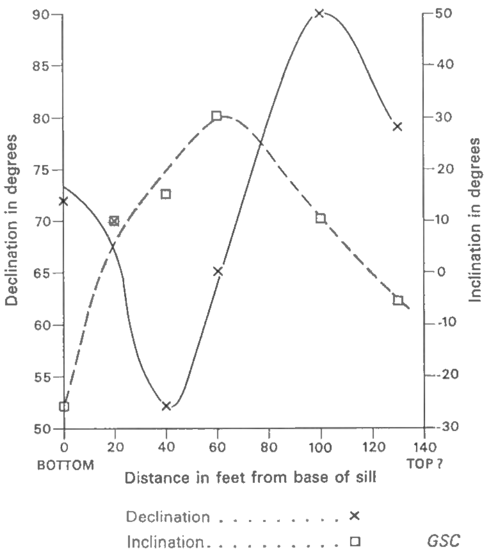

FIGURE 15. Variation of declination and inclination through the sill.

TABLE VIII *Directions across Feeder at Site 21C*

Sample number	Distance from west contact in metres	Initial			A.F. 150			Th. 300°C		
		D	I	M	D	I	M	D	I	M
RN77	0.92	258	+76	297	254	+47	101	191	−46	116
RN30	4.6	116	+86	2420	272	+29	165	215	−15	97
RN32	31.9	254	+45	223	251	+36	94	214	+18	108
RN31	39.2	236	+33	480	219	+42	163	239	− 7	45
RN35	59.2	242	+30	550	236	+36	299	261	+20	218
RN73	77.5	211	+54	8780	239	+37	114	252	−20	181
RN36	95.4	243	+59	526	226	+34	176	284	+10	112
RN74	114	165	+66	—	—	—	—	191	−46	116

D is the declination east of true north. I is the inclination positive downwards. M is the intensity of magnetization in emu $\times 10^{-6}$. The width of the feeder at this point is about 194 metres.

The cooling of the trough-shaped Muskox Intrusion, 5 miles across in the centre, would have been a much longer process. It is likely to have been very complex, and the movement of the isotherms more complicated than any of the cases examined by Jaeger (1961). Cooling from the sides must have been dominant at the deeper, narrower levels. Nevertheless it seems reasonable to assume that in the central layered series, contained by the marginal zone jacket, cooling after consolidation was by conduction upwards towards the surface, so that the *blocking temperature isotherm* would be horizontal and would progress upwards through the layers. Thus the layers provide a time sequence in which layer one was the first layer and layer thirty-four the last to acquire TRM. The time scale is irregular as the layers differ in thickness, and the rate of cooling is not known but is unlikely to differ from that of a thick intrusive sheet (Jaeger, 1958) by more than a factor of two.

Figures 16a and b show the variation of D and I with position in the layered sequence. Only directions have been used from sites in which the resultant vector (R) from two samples was greater than 1.75 (i.e., angular separation less than one radian). Values both after *thermal cleaning* (○one site, ×more than one site) and *magnetic cleaning* (△one site, □more than one site) are plotted if they pass the stability criterion. The directions from layers 17 to 34 after *thermal* and *magnetic cleaning* lie close together: this is considered to indicate stability and the mean D and I of these points from layers where data are available have been joined (Fig. 16). Figures 16a and b show that differences between D and I in different layers are of comparable magnitude to recent changes in the earth's magnetic field caused by *secular variation.* These figures also show that the lower fifteen and uppermost layers give scattered results of low reliability. It might be inferred that the differences in D and I in the central part of the layered series are due to *secular variation* at the time of cooling, of the same order of magnitude as that observed in historic times, and that the mean of these values gives a good estimate of the *dipole field* direction at that time, if one existed.

The lava flows provide another time sequence, the lowermost (site Z) being the oldest. There the lapse of time between flows is unknown and variable and probably of the order of thousands of years, so that the whole sequence may have been extruded over a period of 100,000 years or more. Figure 17 shows D and I plotted against flow number, numbered upwards from the basal flow, using directions of magnetization after *magnetic cleaning* in 75 oe, and rejecting, as before, sites in which R for two specimens was less than 1.75. Directions from each site (a point on Fig. 12f), obtained from two samples taken from the central part of a flow, are thought to give the direction of the field at the instant of time when the blocking temperature isotherm passed through the site. Again the spread in values of D and I is of the same order of magnitude as that caused by recent secular variation superposed on a constant dipole field.

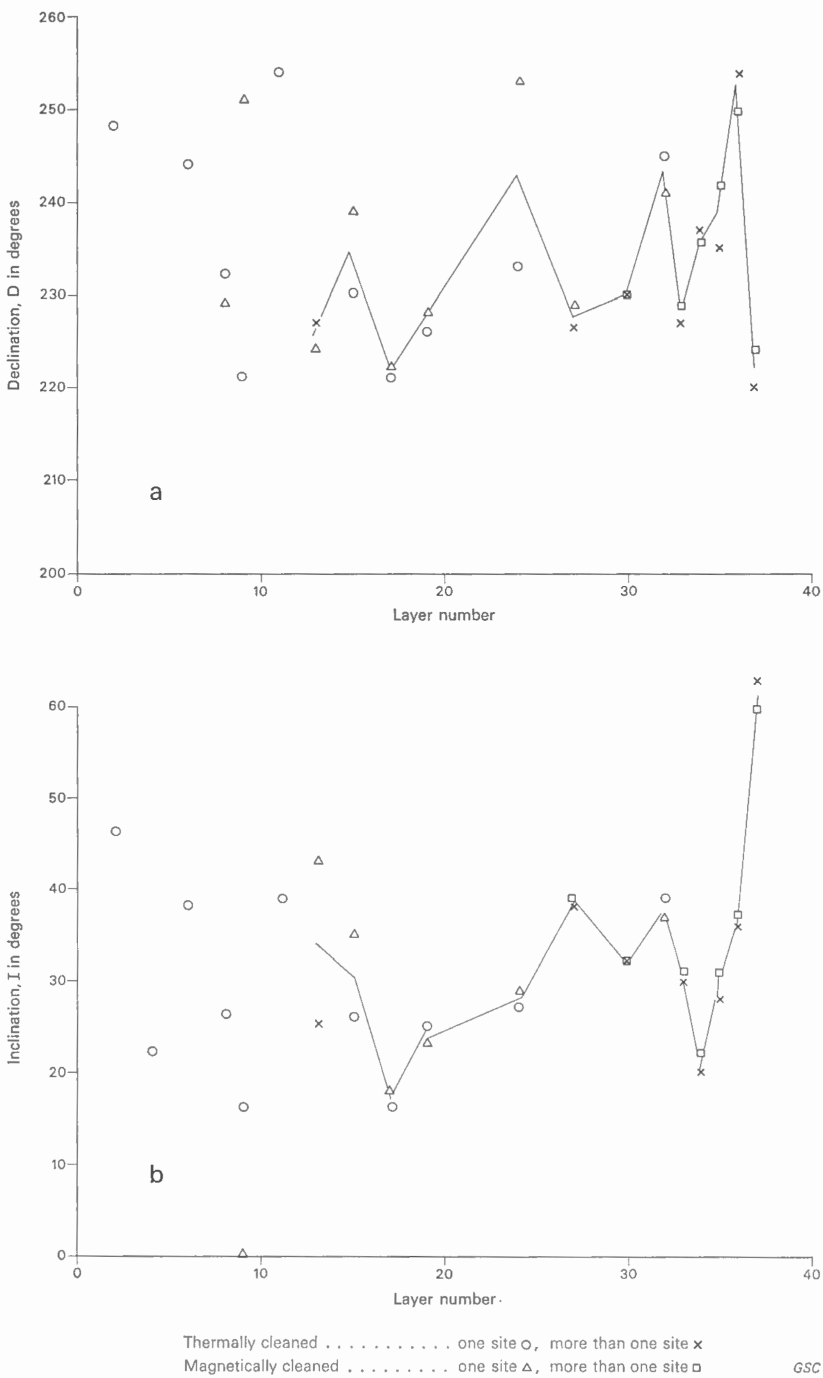

FIGURE 16. Variation of (a) declination and (b) inclination with layer number (1 is the lowest layer) in the central layered series.

Thus we have reconnoitred direction changes on four different time scales; tens of years in the sill, hundreds of years in the *feeder*, thousands of years in the central layered series, and possibly hundreds of thousands of years in the lava sequence. The tentative conclusion is that short period cyclic variations in the ancient field similar to *secular variation* in the recent field affected the earth's magnetic field in Proterozoic time.

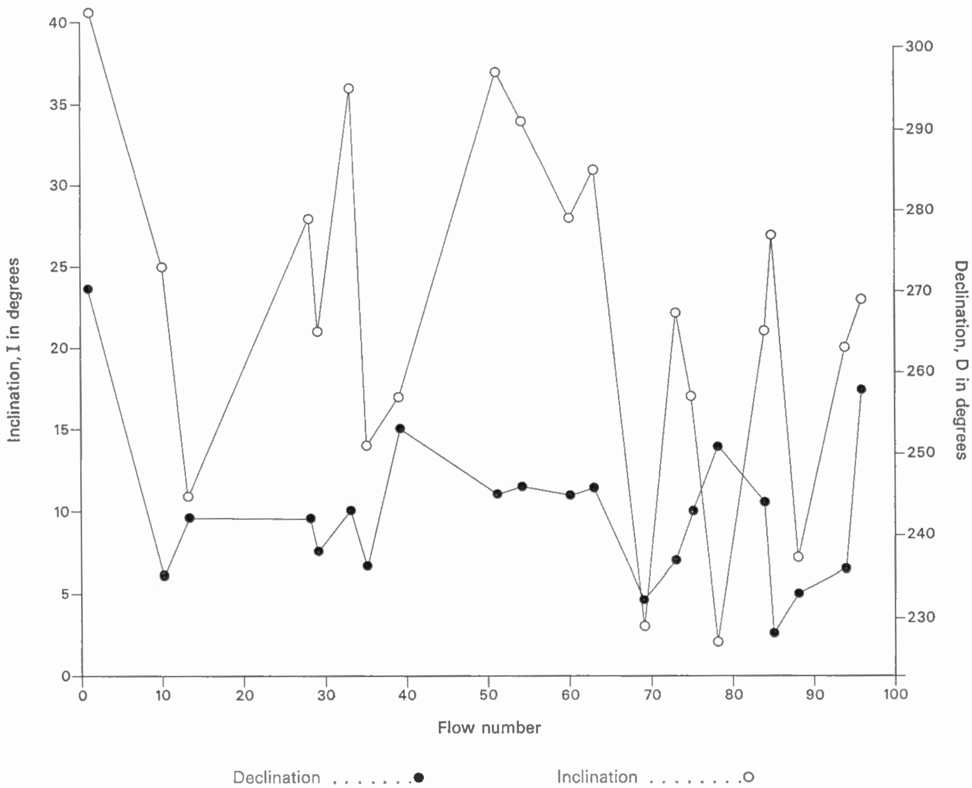

FIGURE 17. Variation of declination and inclination with lava flow number (1 is the oldest flow).

DISCUSSION

This work gives a group of palaeomagnetic pole positions (Fig. 18) obtained from many measurements of directions of magnetization (tested for stability by several methods) from the Coppermine lavas, some dykes from the Mackenzie swarm (No. 7 of Fahrig and Wanless, 1963), and the three major units of the Muskox Intrusion. The results are based on the two assumptions that the magnetization directions from the rock are those of the field at the time of formation and that the earth's magnetic field at that time, when averaged over a few thousand years to smooth cyclic variations, was that of a geocentric dipole. The further assumption that the geocentric dipole was axial, thus relating its direction to the earth's rotation, and so to temperature belts parallel to lines of latitude that broadly control types of sedimentation, opens up the possibility of independent tests of the validity of the assumptions based on the distribution of climatically diagnostic sediments.

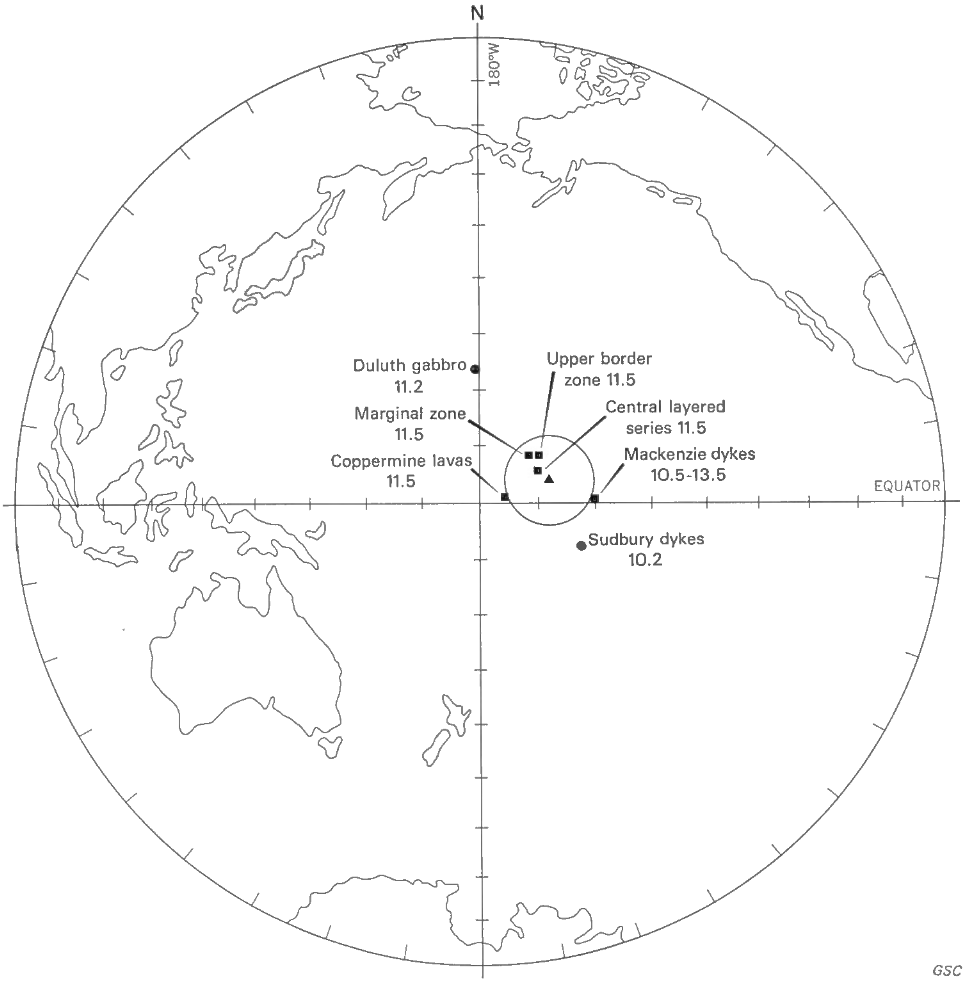

FIGURE 18. An equal-area projection of the Pacific showing radiometrically dated North American Middle Proterozoic pole positions. Ages given in hundreds of millions of years.

In order to relate the pole position to a particular epoch it is necessary to know the age of the rock from which it was derived. Radiogenic methods give the most reliable dates for Precambrian rocks, but in the age range of 1,000 to 1,300 m.y. there is an uncertainty of more than 100 m.y. (Leech, *et al.,* 1963).

Apart from the results given here, the only Middle Proterozoic formations from North America for which both radiogenic ages and pole positions have been determined are the Duluth gabbro (Du Bois, 1962) and the Sudbury diabase dykes (Sopher, 1963), although data from other dyke swarms in the Canadian Shield should be available shortly (E. H. S. Gaucher, pers. com.). The preliminary results of Du Bois (1960, 1962) and Collinson and Runcorn (1960) lack both radiogenic age determinations and detailed stability studies, and are not used here.

The Sudbury diabase dykes have yielded radiogenic ages of 1,020 m.y. (Fairbairn, *et al.,* 1960) and 1,220 m.y. (Fahrig and Wanless, 1963), and the age range of the Duluth gabbro has been determined as 1,080 to 1,200 m.y. (Goldich, *et al.,* 1961). These ages are similar to those of the formations studied here and the pole positions derived from them are shown in Figure 18. The number of samples from the Sudbury diabase dykes is, however, too small to yield a reliable result, and there is a possibility that the Duluth gabbro pole position is affected by secondary components as the specimens were not *cleaned* in the laboratory. The mean pole for the late Middle Proterozoic (▲ of Fig. 18), therefore, has been computed using only three units of the Muskox Intrusion, the Mackenzie dykes, and the Coppermine lavas, giving each unit weight.

The radiogenic ages indicate that all these formations are between 1,000 and 1,300 m.y. old. The agreement between the poles (Fig. 18) suggests that there has been no significant polar wandering between the time of formation of the Coppermine lavas, the Mackenzie dykes, and the Muskox Intrusion. The mean position of the pole for late Middle Proterozoic time calculated from the five major units used here after *magnetic cleaning* in a peak alternating field of 75 oe is (4.7°N, 191.2°E; $k = 90$, $R = 4.957$, $\alpha = 8$).

The Middle Proterozoic palaeolatitude lines for North America shown in Figure 19 have been constructed from this pole position. The meridional attitude of these palaeolatitude lines suggests that rock types that are typical of warm regions, such as desert sandstones, salt deposits, and massive limestones, should form a meridional belt down eastern North America. Thus evaporites in the Middle Proterozoic of the Canadian Arctic would confirm these lines, whereas glacial formations would refute them, unless the glacial deposits could be shown to be part of a world-wide ice age such as that postulated by Harland and Rudwick (1964). The occurrence of gypsum and anhydrite in the Minto Inlet Formation of Victoria Island (Thorsteinsson and Tozer, 1962), is consistent with the low palaeolatitude of the island indicated in Figure 19.

These results encourage belief in the possibility of palaeomagnetic dating of major Precambrian events. The first step is to obtain a polar wandering curve underpinned by directions that have been tested for stability from formations that yield a group of concordant radiogenic ages. This work gives a point on the curve

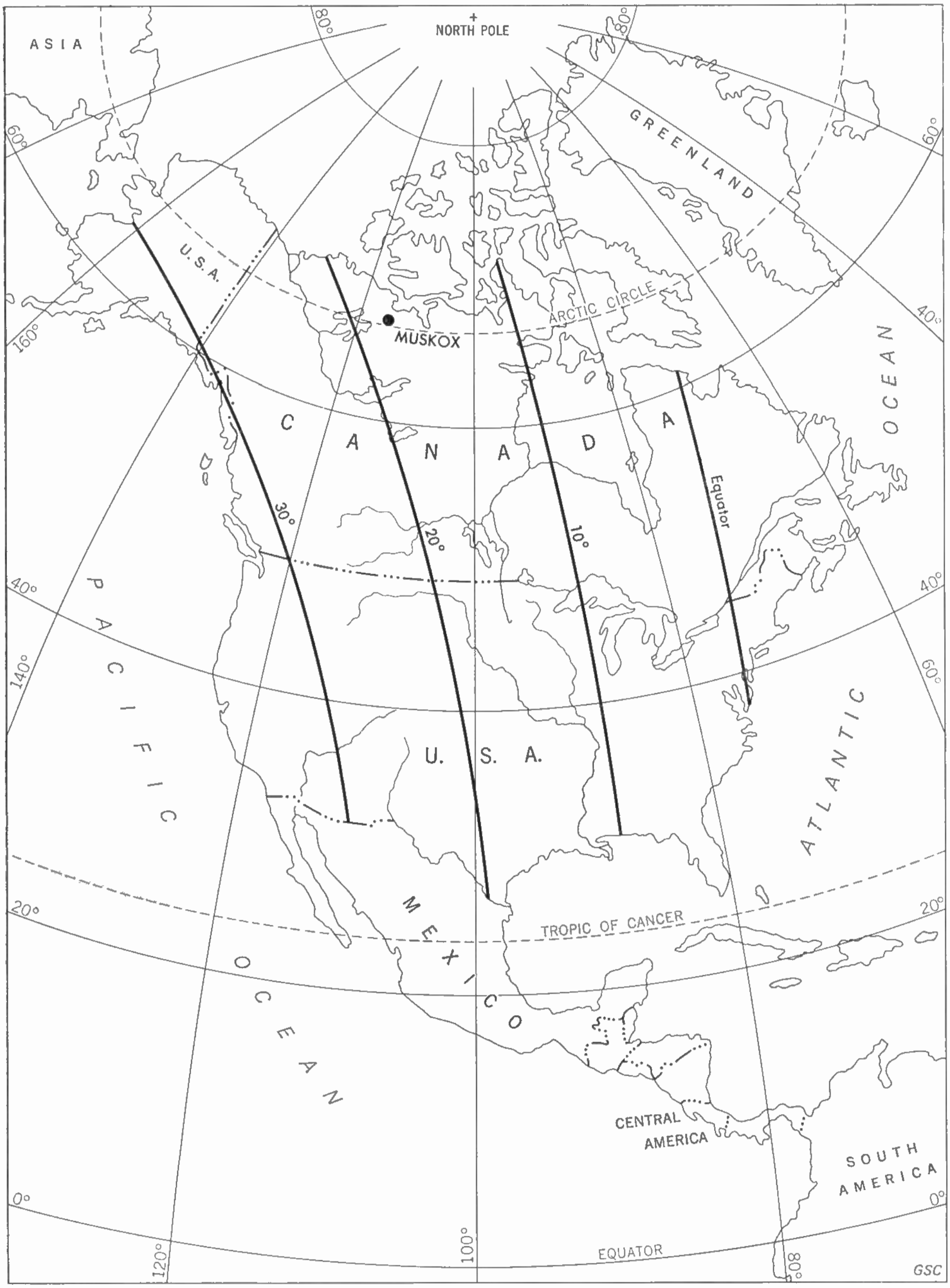

FIGURE 19. Late Middle Proterozoic palaeolatitude map for North America based on pole positions derived in this bulletin.

for the late Middle Proterozoic. This point may be tested geologically by comparing the distribution of temperature-dependent rock types of the period with the palaeolatitude lines.

When the curve can be drawn from reliable data, pole positions from formations of unknown age may be fitted to it and thus, within the limits of the data, be assigned a palaeomagnetic age. Finally, the polar wandering curve for North America may be compared with similar curves from other continents to help to solve major structural problems in the earlier history of the earth.

REFERENCES

Akimoto, S.

1955: Magnetic properties of ferromagnetic minerals contained in igneous rocks; *Jap. J. Geophys.*, vol. 1, pp. 1–31.

1957: Magnetic properties of ferromagnetic oxide minerals as a basis of rock magnetism; *Phil. Mag.*, vol. 6, pp. 288–298.

Bruhnes, B.

1906: Recherche sur la direction d'aimantation des roches volcaniques; *J. Phys.*, vol. 5, pp. 705–724.

Burwash, R. A., Baadsgaard, H., Campbell, F. A., Cumming, G. L., and Folinsbee, R. E.

1963: Potassium-argon dates of diabase dyke systems, District of Mackenzie, N.W.T.; *Bull. Can. Min. Metall.*, vol. 66, pp. 303–307.

Chevallier, R.

1925: L'aimantation des laves de l'Etna et l'orientation du champ terrestre en Sicile du XII^e au XVII^e siècle; *Ann. Phys.*, Ser. 10, pp. 4–152.

Collinson, D. W., and Runcorn, S. K.

1960: Polar wandering and continental drift: evidence from palaeomagnetic observations in the United States; *Bull. Geol. Soc. Amer.*, vol. 71, pp. 915–958.

Cox, A.

1961: Anomalous remanent magnetization of basalt; *U.S. Geol. Surv.*, Bull. 1083-E., pp. 131–160.

Creer, K. M.

1957: Remanent magnetization of unstable Keuper marls; *Phil. Trans. Roy. Soc. London*, Ser. A, vol. 250, pp. 130–143.

Creer, K. M., Irving, E., and Runcorn, S. K.

1957: Geophysical interpretation of palaeomagnetic directions from Great Britain; *Phil. Trans. Roy. Soc. London*, Ser. A, vol. 250, pp. 144–156.

Doell, R. R., and Cox, A.

1963: The accuracy of the palaeomagnetic method as evaluated from historic Hawaiian lava flows; *J. Geophys. Res.*, vol. 68, pp. 1997–2009.

Du Bois, P.M.

1960: Correlation of Keweenawan rocks of Lake Superior District by palaeomagnetic methods; *Proc. Geol. Assoc. Can.*, vol. 11, pp. 115–128.

1962: Palaeomagnetism and correlation of Keweenawan rocks; *Geol. Surv. Can.*, Bull. 71.

Fahrig, W. F., and Wanless, R. K.
1963: Age and significance of diabase dyke swarms of the Canadian Shield; *Nature,* vol. 200, pp. 934–937.

Fairbairn, H. W., Hurley, P. M., and Pinson, W. H.
1960: Mineral and rock ages at Sudbury–Blind River, Ontario; *Proc. Geol. Assoc. Can.,* vol. 12, pp. 41–66.

Findlay, D. C., and Smith, C. H.
1965: The Muskox drilling project; *Geol. Surv. Can.,* Paper 64–44.

Fisher, R. E.
1953: Dispersion on a sphere; *Proc. Roy. Soc. London,* Ser. A, vol. 217, pp. 295–305.

Fraser, J. A.
1960: North-central District of Mackenzie, Northwest Territories; *Geol. Surv. Can.,* Map 18-1960.

Fuller, M. D.
1960: Anisotropy of susceptibility and the natural remanent magnetization of some Welsh slates; *Nature,* vol. 186, pp. 791–792.
1963: Magnetic anisotropy and palaeomagnetism; *J. Geophys. Res.,* vol. 68, pp. 293–309.
1964: On the magnetic fabric of certain rocks; *J. Geol.,* vol. 72, pp. 368–376.

Goldich, S. S., Nier, A. O., Baadsgaard, H., Hoffman, J. H., Krueger, H. W.
1961: The Pre-Cambrian geology and geochronology of Minnesota; *Univ. Minnesota, Minnesota Geol. Surv.,* Bull. 41.

Graham, J. W.
1949: The stability and significance of magnetism in sedimentary rocks; *J. Geophys. Res.,* vol. 54, pp. 131–167.

Graham, K. W. T.
1961: The re-magnetization of a surface outcrop by lightning strikes; *Geophys. J.,* vol. 6, pp. 85–102.

Granar, L.
1958: Magnetic measurements of Swedish varved sediments; *Arkio för Geofysik,* vol. 3, pp. 1–40.

Griffiths, D. H., King, R. F., Rees, A. I., and Wright, A. E.
1960: The remanent magnetism of some recent varved sediments; *Proc. Roy. Soc. London,* Ser. A, vol. 256, pp. 359–383.

Harland, W. B., and Rudwick, M. J. S.
1964: The Infra-Cambrian ice age; *Scient. Amer.,* vol. 211, pp. 28–36.

Howell, L. G.
1962: Chemical and crystal controlled magnetization of rocks; *Am. J. Sci.,* vol. 260, pp. 539–549.

Howell, L. G., Martinez, J. D., Frosch, A., and Statham, E. H.
1960: A note on chemical magnetization of rocks; *Geophysics,* vol. 25, pp. 1094–1099.

Irving, E.
1964: Palaeomagnetism and its application to geological and geophysical problems; Wiley and Sons, pp. 1–399.

Irving, E., Robertson, W. A., Stott, P. M., Tarling, D. H., and Ward, M. A.
1961: Treatment of partially stable sedimentary rocks showing planar distributions of directions of magnetization; *J. Geophys. Res.,* vol. 66, pp. 1927–33.

Jaeger, J. C.

1957: The temperature in the neighborhood of a cooling intrusive sheet; *Am. J. Sci.*, vol. 255, pp. 306–318.

1958: The solidification and cooling of intrusive sheets; *Dolerite Symposium, Hobart,* July 1957, pp. 77–87.

1961: The cooling of irregularly shaped igneous bodies; *Am. J. Sci.*, vol. 259, pp. 721–734.

Jaeger, J. C., and Green, R.

1956: The use of the cooling history of thick intrusive sheets for the study of the secular variation of the earth's magnetic field; *Geofis. pur. appl.*, vol. 35, pp. 49–53.

Johnson, E. A., Murphy, T., and Torreson, O. W.

1948: Pre-history of the earth's magnetic field; *Terr. Mag.*, vol. 53, pp. 349–372.

Kern, J. W.

1961a: Effects of moderate stresses on directions of thermoremanent magnetization; *J. Geophys. Res.*, vol. 66, pp. 3801–3805.

1961b: Stress stability of remanent magnetization; *J. Geophys. Res.*, vol. 66, pp. 3817–3820.

Kobayashi, K.

1959: Chemical remanent magnetization of ferromagnetic minerals and its application to rock magnetism; *J. Geomag. Geoelec.*, vol. 10, pp. 99–117.

Larochelle, A.

1958: A study of the palaeomagnetism of rocks from Yamaska and Brome Mountains, Que.; McGill Univ., Montreal, unpub. Ph.D. thesis.

1964: Geological solar compass; *Geol. Surv. Can.*, Paper 62-2, pp. 44–47.

1965: The design of a spinner type remanent magnetometer; *Geol. Surv. Can.*, Paper 64-43.

Leech, G. B., Lowdon, J. A., Stockwell, C. H., and Wanless, R. K.

1963: Age determinations and geological studies; *Geol. Surv. Can.*, Paper 63-17.

Lowdon, J. A.

1961: Age determinations by the Geological Survey of Canada; *Geol. Surv. Can.*, Paper 61-17, p. 22.

McElhinny, M. W., and Gough, D. I.

1963: The palaeomagnetism of the Great Dyke of Southern Rhodesia; *Geophys. J.*, vol., 7, pp. 287–303.

Neél, L.

1955: Some theoretical aspects of rock magnetism; *Adv. in Phys.*, vol. 4, pp. 191–242.

Nicholls, G. D.

1955: The mineralogy of rock magnetism; *Adv. in Phys.*, vol. 4, pp. 113–190.

Robertson, W. A.

1963a: A palaeomagnetic study of igneous rocks from Eastern Australia; Australian National Univ., Canberra, Ph.D. thesis.

1963b: Palaeomagnetism of some Mesozoic intrusives and tuffs from Eastern Australia; *J. Geophys. Res.*, vol. 68, pp. 2299–2312.

1964a: Construction of a non-magnetic oven; *Geol. Surv. Can.*, Paper 64-2, pp. 51, 52.

1964b: Palaeomagnetic results from northern Canada suggesting a tropical Proterozoic climate; *Nature*, vol. 204, pp. 66, 67.

Roy, J. L.
1963: The measurement of the magnetic properties of rock specimens; *Pubs. Dom. Obs.*, vol. 27, pp. 421–439.

Smith, C. H.
1962: Notes on the Muskox Intrusion, Coppermine River area, District of Mackenzie; *Geol. Surv. Can.*, Paper 61-25, pp. 1–16.

Smith, C. H., and Kapp, H. E.
1963: The Muskox Intrusion, a recently discovered layered intrusion in the Coppermine River area, Northwest Territories, Canada; *Min. Soc. Am.*, Spec. Paper 1, pp. 1–35.

Sopher, S. R.
1963: Palaeomagnetic study of the Sudbury Irruptive; *Geol. Surv. Can.*, Bull. 90, pp. 1–26.

Stacey, F. D.
1960a: Stress-induced magnetic anisotropy of rocks; *Nature,* vol. 188, pp. 134, 135.
1960b: Magnetic anisotropy of igneous rocks; *J. Geophys. Res.*, vol. 65, pp. 2429–2442.
1963: The physical theory of rock magnetism; *Adv. in Phys.*, vol. 12, pp. 45–133.

Stacey, F. D., Joplin, G., and Lindsey, J.
1960: Magnetic anisotropy and fabric of some foliated rocks from S. E. Australia; *Geofis, pur. appl.*, vol. 47, pp. 30–40.

Stott, P. M., and Stacey, F. D.
1959: Magnetostriction and palaeomagnetism of igneous rocks; *Nature,* vol. 183, pp. 384–385.
1960: Magnetostriction and palaeomagnetism of igneous rocks; *J. Geophys. Res.*, vol. 65, pp. 2419–2424.
1961: Stress effects on thermoremanent magnetization; *Nature,* vol. 191, pp. 585–586.

Thellier, E.
1937: Sur l'aimantation dite permanente des basaltes; *C.R. Acad. Sc.*, vol. 204, pp. 876–879.

Thorsteinsson, R., and Tozer, E. T.
1962: Banks, Victoria, and Stefansson Islands, Arctic Archipelago; *Geol. Surv. Can.*, Mem. 330.

Torreson, O. W., Murphy, T., and Graham, J. W.
1949: Magnetic polarization of sedimentary rocks and the earth's magnetic history; *J. Geophys. Res.*, vol. 54, pp. 111–129.

Vincent, E. A., Wright, J. B., Chevallier, R., and Mathieu, S.
1957: Heating experiments on some natural titaniferous magnetites; *Min. Mag.*, vol. 31, pp. 624–655.

Wanless, R. K., Stevens, R. D., Lachance, G. R., and Rimsaite, J. Y. H.
1965: Age determinations and geological studies: Part I: Isotopic Ages, Report 5; *Geol. Surv. Can.*, Paper 64-17.
1966: Age determinations and geological studies: Part I: Isotopic Ages, Report 6; *Geol. Surv. Can.*, Paper 65-17.

Watson, G. S.
1956: A test of randomness of directions; *Geophys. Supp.*, vol. 7, pp. 160–161.

Watson, G. S., and Irving, E.
1957: Statistical methods in rock magnetism; *Geophys. Supp.*, vol. 7, pp. 289–300.

BULLETINS

Geological Survey of Canada

Bulletins present the results of detailed scientific studies on geological or related subjects. Some recent titles are listed below (Queen's Printer Cat. No. in brackets):

151 Precambrian geology of Boothia Peninsula, Somerset Island, and Prince of Wales Island, District of Franklin, *by* R. G. Blackadar, 1967, $2.25 (M42-151)

152 Lower Cretaceous Bullhead and Fort St. John Groups, between Smoky and Peace Rivers, Central Rocky Mountain Foothills, Alberta and British Columbia, *by* D. F. Stott, 1968, $7.00 (M42-152)

153 Lower and Middle Devonian Trilobites of the Canadian Arctic Islands, *by* A. R. Ormiston, 1967, $5.50 (M42-153)

154 Deglaciation studies in Kamloops region, an area of moderate relief, B.C., *by* R. J. Fulton, 1968, $2.00 (M42-154)

155 Middle and Upper Triassic spiriferinid brachiopods from the Canadian Arctic Archipelago, *by* A. Logan, 1967, $2.00 (M42-155)

156 A standard for Triassic time, *by* E. T. Tozer, 1967, $4.00 (M42-156)

157 Lower Palaeozoic sediments of northwestern Baffin Island, *by* H. P. Trettin, 1968, $2.00 (M42-157)

158 Hettangian ammonite faunas of the Taseko Lakes area, B.C., *by* Hans Frebold, 1967, $2.00 (M42-158)

159 Study of pegmatite bodies and enclosing rocks, Yellowknife-Beaulieu region, District of Mackenzie, *by* R. Kretz, 1968, $3.00 (M42-159)

160 The geochemistry of silver and its deposits, *by* R. W. Boyle, 1968, $6.50 (M42-160)

161 Petrology and structure of Nakusp map-area, British Columbia, *by* D. W. Hyndman, 1968, $2.75 (M42-161)

162 The pyroxene granulites of the Mount Wright map-area, Quebec–Newfoundland, *by* R. A. Roach and Stanley Duffell, 1968, $2.50 (M42-162)

163 Contributions to Canadian palaeontology: Lower Cambrian faunas from Ellesmere Island, District of Franklin, *by* J. W. Cowie; a Middle Cambrian *Plagiura-Poliella* faunule from southwest District of Mackenzie, *by* B. S. Norford, 1968, $1.75 (M42-163)

164 Silurian cephalopods of James Bay lowland, with a revision of the Family Narthecoceratidae, *by* R. H. Flower, 1968, $5.00 (M42-164)

165 Contributions to Canadian palaeontology: Conodonts and fish remains from the Stonehouse Formation, Arisaig, Nova Scotia, *by* Jocelyne A. Legault; Osteostraci from Somerset Island, *by* D. L. Dinely; A Devonian Osteolepidid fish from British Columbia, *by* H. Jessen, 1968, $2.50 (M42-165)

167 Magnetization directions in the Muskox Intrusion and associated dykes and lavas, *by* W. A. Robertson, 1969, $1.50 (M42-167)